Federal University of São Carlos
Graduate Program in Physics
Center for Exact Sciences and Technology

Spin Dynamics in Exciton Behavior

Student: Jhon F. Contreras
Advisor: Prof. Victor Lopez-Richard

Thesis for
Master in Physics.

Masters thesis submitted to the Graduate Program of Physics at the Federal University of São Carlos, in partial fulfillment of the requirements for obtaining the degree of Master of Science in Physics.

November

2023

Spin Dynamics in Exciton Behavior

Members of the Examining Bench:

Thesis advisor:	_____
Dr. Victor Lopez Richard	Firma
Examiner Name:	_____
Dr. Anibal Thiago Bezerra	Firma
Examiner Name:	_____
Dr. Matheus Paes Lima	Firma

Defense Date: November 30, 2023

Acknowledgements

I would like to express my sincere gratitude to Professor Victor Lopez-Richard for his invaluable contribution to the completion of this master's thesis in physics. His help, patience, and dedicated guidance were essential in this arduous process.

Without his experience and guidance, this academic achievement would not have been possible. Every interaction with Professor Victor represented a valuable lesson and learning opportunity. Professor's ability to explain complex concepts clearly and address my questions patiently has been truly inspiring.

The trust placed in me and the commitment demonstrated to my academic development have left a lasting mark. I sincerely appreciate the opportunity to have worked under the direction of Professor Victor and I am sure that the lessons learned will be fundamental in my professional career.

This achievement is not only mine, but also that of Professor Victor, whose positive influence has left a significant mark on my academic training.

I must also mention the essential help of the Coordination of Superior Level Staff Improvement (CAPES), without whose financial support it would not have even been imaginable for me to access studies at this level of training, for which I present my deep respect and gratitude. I also acknowledge the support of the Graduate Program in Physics at the Federal University of Sao Carlos (UFSCar), without whose resources, trust and diligence, this work would not have been possible.

With all my respect and deep gratitude,
Jhon F. Contreras

Abstract

This thesis presents a study on the spin dynamics of confined excitons under the influence of a magnetic field. Experimental observations reveal unique correlations between Zeeman splitting and spin thermalization, which can be tuned to both temperature and incident light power. The theoretical model, which considers the eventual spin thermalization of bright excitons, qualitatively agrees with the experimental observations and highlights the importance of the exchange interaction. Furthermore, this study goes beyond previous approaches, offering additional insights into spin relaxation and the effects of correlations between bright and dark excitons. Two fundamental conclusions are derived from this work: first, it is shown that the spin dynamics of excitons confined under a magnetic field can be tuned by both temperature and incident power. Second, it is noted that the polarization of the electrons is not appropriate to adjust the experimental curve of the degree of optical polarization, since under the same approximations it is obtained that the optical polarization is zero. These conclusions provide valuable insights for interpreting experimental measurements and guiding future investigations into the spin dynamics of excitons in confinement.

Resumo

Esta tese apresenta um estudo sobre a dinâmica de spin de éxcitons confinados sob a influência de um campo magnético. Observações experimentais revelam correlações únicas entre a divisão de Zeeman e a termalização de spin, que podem ser ajustadas tanto à temperatura quanto à potência da luz incidente. O modelo teórico, que considera a eventual termalização do spin de excitons brilhantes, concorda qualitativamente com as observações experimentais e destaca a importância da interação de troca. Além disso, este estudo vai além das abordagens anteriores, oferecendo insights adicionais sobre o relaxamento do spin e os efeitos das correlações entre excitons claros e escuros. Duas conclusões fundamentais são derivadas deste trabalho: primeiro, é mostrado que a dinâmica de spin dos excitons confinados sob um campo magnético pode ser ajustada tanto pela temperatura quanto pela potência incidente. Em segundo lugar, nota-se que a polarização dos elétrons não é adequada para ajustar a curva experimental do grau de polarização óptica, pois sob as mesmas aproximações obtém-se que a polarização óptica é zero. Estas conclusões fornecem informações valiosas para a interpretação de medições experimentais e orientar futuras investigações sobre a dinâmica de spin de excitons em confinamento.

I INTRODUCTION **9**

II Experimental motivation **11**

III OBJECTIVES **14**

IV Theoretical background **15**

A Electronic structure of semiconductors 15

B Excitons 18

C Optical selection rules and circularly polarized light. 19

D Hamiltonian exciton in a quantum well 21

E Density of states 2D 22

F Electron-hole exchange interaction 23

V Incoherent processes **34**

A Radiative 34

B Non-Radiative 35

C Spin Flip 36

D Photogeneration 37

E Final Expressions 37

VI Results **44**

A Spin polarization 44

B Termalization 49

VII Conclusions **60**

References **61**

I. INTRODUCTION

Photoluminescence (PL) consists in the emission of light from a system when it is exposed to electromagnetic radiation. It may take place in a variety of materials, including inorganic solids, organic molecules, semiconductors, and nanoscopic devices, providing information about their electronic structure and other physical properties. When a photon with sufficient energy is absorbed by a semiconductor or other luminescent material, it excites electrons to higher energy states. As these electrons return to their original energy states, they release energy in the form of light [1]. The wavelength and intensity of the emitted light can then be used to determine the energy levels of the electrons in the material and the effectiveness of the photoluminescence process, respectively. By using adequate excitation and detection configurations it can also provide information about the spin degrees of freedom of the electronic states that have significant effects on the physical and chemical properties of materials. The spin of an electron in a nanostructure affect the way it responds to magnetic fields, or different temperatures [2], which in turn can impact the material's electrical conductivity and other physical properties. It is indeed the study of spin properties of nanostructures and how they respond to the absorption and emission of light the main focus of the present project.

Understanding the spin-properties of nanostructures [3] can be useful to develop new technologies , such as spintronics[4], which use the spin of electrons for computing architectures instead the traditional logic transistors [5]. The spin of an electron in a nanostructure can be modulated by temperature through thermal changes, which can cause the spin to become more or less aligned with an external magnetic field. In some cases the spin of an electron becomes more sensitive to thermal fluctuations at higher temperatures, which can lead to changes in the semiconductor magnetic properties. The presence of high-energy photons can also excite electrons, causing their spins to

become more or less aligned with an external magnetic field.

When studying electronic, spin, and optical properties in solid state physics it is unavoidable to introduce quasi particles that describe collective interactions reducing them to single or few particles representations. Specifically excitons, that represent an electronic state of electrons in the conduction band and their paired vacancies in the valence band (holes), are relevant when dealing with inter-band transitions mediated by light absorption and emission. Excitons are made up of an electron and a hole, each with its own spin, and the exchange coupling between them plays a critical part in their collaborative behavior [6].

The exchange interaction in solids refers to the quantum mechanical effect that arises from the Pauli exclusion principle, influencing the behavior of electrons within a crystalline lattice. It is a fundamental concept in condensed matter physics and plays a crucial role in determining the magnetic properties of materials. It can be defined as the quantum-mechanical interaction energy associated with the exchange of identical particles, such as electrons, in a many-body system. According to the Pauli exclusion principle, which establishes that two electrons in an atom cannot have all their quantum numbers identical, that is, in our case, the electrons with the same spin cannot occupy the same quantum state simultaneously. The exchange interaction arises from the anti symmetry of the wave function for identical particles, leading to a repulsive energy when electrons are in close proximity with parallel spins and an attractive energy when spins are anti parallel [7].

In the context of solids, the exchange interaction contributes to the formation of magnetic moments and the alignment of electron spins, giving rise to various magnetic phenomena such as ferromagnetism, antiferromagnetism, and ferrimagnetism. The strength [4] and nature of the exchange interaction depend on the specific arrangement of atoms and electrons in the crystal lattice, as well as the material's electronic structure.

There is a variety of ways where traces of the exchange coupling emerge, for instance through excitation at two close energy levels that results in two close but different

frequencies. This leads to an interference between them and a modulation of the emitted light polarization provoking beats [8] that reflect the exciton spin splitting in the transverse magnetic field into two different states: bright excitons and dark excitons.

In our work we study in the first instance how excitons confined in a quantum dot behave when exposed to an external magnetic field, giving rise to the polarization of the excitons, as proposed in the recent study by Smirnov [9] , and as observed by our experimental colleagues at UfScar, who measured the degree of circular polarization in an InAs/GaAsSb sample, and observed an interesting relationship with the polarization of the electrons as we will discuss later. For that study we reproduced the calculations from the paper and extended its ideas to understand the nature of the degree of circular polarization in the material.

We also carried out the calculation of the Zeeman splitting taking into account that it could have a strong influence with the distribution of the up and down spins for the electrons and holes in the semiconductor, with which we obtained a good model to understand the atypical behavior observed in the measurements carried out by our colleagues.

II. EXPERIMENTAL MOTIVATION

Understanding how the temperature impacts the dynamics of the spins confined in nanostructures and how the incident power of a laser beam can be used to manipulate their magnetic response are goals of the present Master Thesis, as some studies suggest the possibility of control the spin behavior on the magnetic field is known [10] [2]. In order to resolve the spin nature of the transitions that induce the emission of photons it is necessary to use circularly polarized light given the selection rules that control the optical excitation and recombination, described later.

In polarization resolved PL experiments carried out by experimental colleagues at the Physics Department at UFSCar in InAs/GaAsSb quantum dots they have been

able to identify a non-monotonic modulation of the degree of circular polarization (DCP) [11] as represented in Fig.1, for a sample kept out of equilibrium via energy pumping and cooling simultaneously. These experimental results have been fitted with a theoretical model for electron polarization described in Ref. [9]. Yet, it is the scope of this thesis to corroborate or not whether such an interpretation is feasible.

Our colleagues have also been able to resolve the energy splitting of spin states (Zeeman effect) in InGaAs quantum wells in the presence of an external magnetic field. Part of these results have been summarized in Fig. 2. Note, in the left panel, that the absolute value of energy splitting grows with magnetic field for high illumination powers, yet the monotonic behavior changes drastically for low powers. An analogous effect has been presented in the right panel by reducing the temperature.

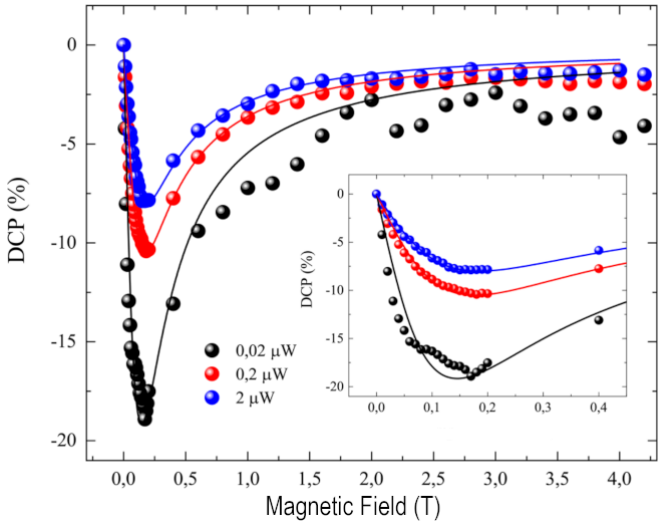

FIG. 1: Degree of circular polarization measured at 4K in InAs/GaAsSb quantum dots as a function of the applied magnetic field for various intensities of the incident light. Adjustment of experimental data in the region of dynamic spin polarization, with the inset expanding the region of low magnetic fields [12]

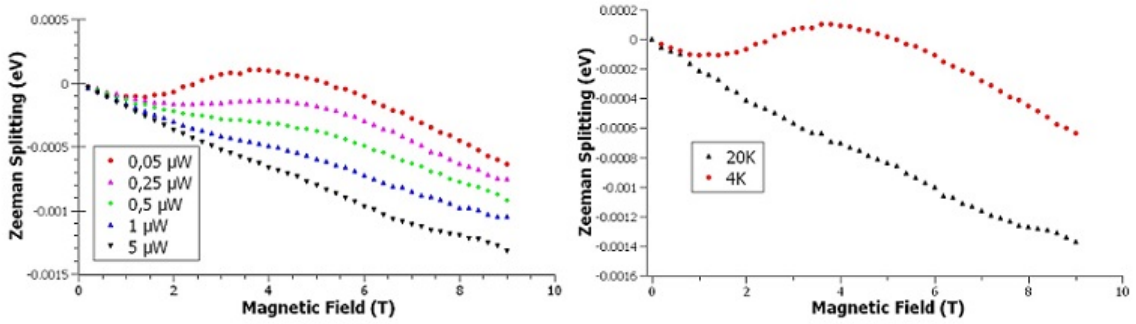

FIG. 2: Zeeman splitting of electron-hole pairs detected in the Photoluminescence of InGaAs quantum wells under an applied magnetic field. Left panel: various incident power of the incoming light at a fixed temperature. Right panel: the results for two different temperatures under the same incident power. Results provided by the experimental colleagues.

Thus, relevant scientific questions can be raised: what is the nature of these effects and how to be able to modulate them. Given that there is a clear correlation with the occupation of spin states that can be controlled by the incoming intensity and temperature a relevant hypothesis to be tested is the eventual effect of the exchange interaction and the magnetic field tuning of the spin relaxation, because the excitonic effect and other effects that do not depend on spin have a negligible contribution to understanding the phenomenon. Also relevant, the spin-relaxation, that is the process by which the spin state of an electron in a semiconductor structure becomes randomized due to interactions with the crystal lattice or other electrons, must be considered. There are several mechanisms that contribute to it including the Elliott- Yafet mechanism [13], the D'yakonov-Perel mechanism, and the Bir-Aronov-Pikus [14] mechanism. In turn, exchange effects related to indistinguishable interacting electrons in the solid, can be reduced to the effective interactions between their spins. This affect the energy of configurations of aligned or anti-aligned of the spins in particular of electron-hole pairs as described previously. These excitons can be classified as bright or dark, depending on their spin properties. Bright excitons are those in which the spin of the electron and hole are aligned, allowing for a direct recombination emitting light, whereas dark

ones are those in which the spin of the electron and hole are anti-aligned, where such a recombination is forbidden (at least in the first order approximation in perturbation theory). The interplay between the spin relaxation, magnetic fields, and exchange interactions can affect the relative populations of bright and dark excitons which can in turn affect the overall spin dynamics of the system.

III. OBJECTIVES

Given these premises as motivations for the current thesis, a set of scientific tasks was programmed according to the following objectives:

1. Develop and strengthen research and analytical skills by employing mathematical and computational techniques in semiconductor physics, providing hands-on experience in conducting independent research, data analysis, and critical interpretation of results and available literature.

2. Explore and characterize the electronic and optical properties of confined excitons under the dynamic conditions of continuous light pumping and the effect of spin relaxation and exchange interaction.

3. Investigate the role of thermalization and the interplay with exchange interaction in the exciton emission.

The scientific tasks are devoted to two main problems related to exciton spin and exchange interaction: one demands the use of a stationary model where thermal equilibrium can be assumed yet another requires a dynamic approach.

In addition to becoming familiar with the fundamentals of semiconductor theory, a concrete milestone was established and achieved in order to address the main scientific questions raised: reproducing the results summarized in Physical Review Letters 125, 156801 (2020), Ref. [9], with the purpose of verifying the dynamic spin effects on the modulation of exciton spin polarization for the non-equilibrium system and contrast this with the experimental results just presented.

IV. THEORETICAL BACKGROUND

A. Electronic structure of semiconductors

When the interaction between radiation and matter is studied, simple approaches such as two-level models are usually used, in which after interacting with an electromagnetic field, transitions of electrons are induced from one level to another, however in the case of semiconductors, we are not only talking about two allowed energy levels, but also energy bands. Semiconductors are extremely widely used materials both in solid-state physics research [15] and in practically any modern electronic device. A useful and many times reasonable approximation for the description of the band structure of semiconductors is the assumption of parabolic relations in momentum space of the main energy states involved in certain phenomena as represented in Fig. 3 (Left). This simplifies the mathematical description and makes it easier to calculate both optical and transport properties.

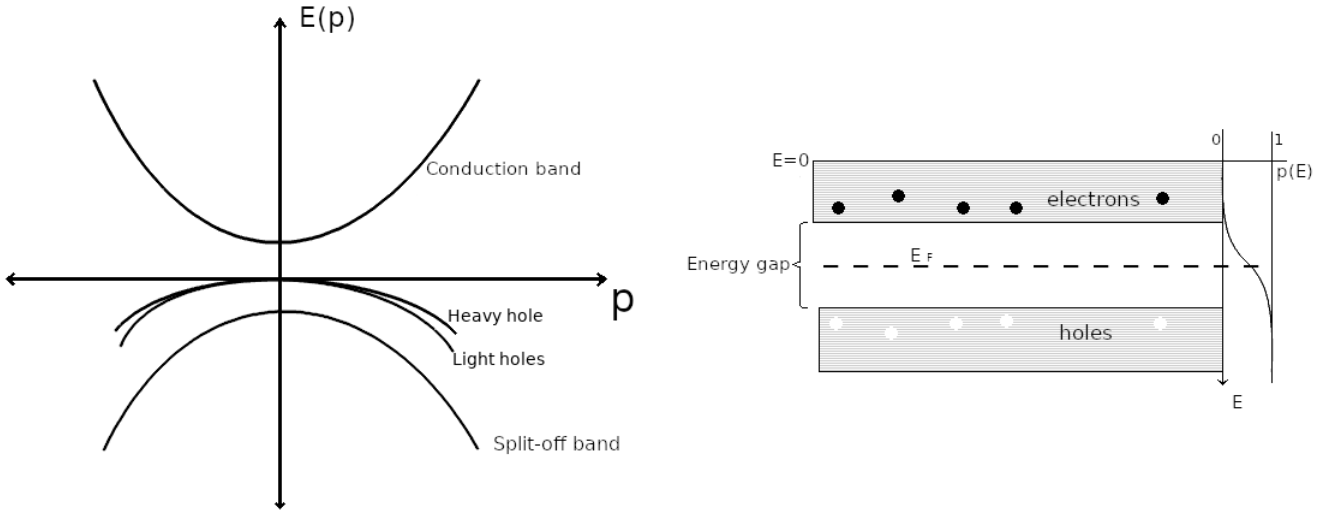

FIG. 3: (Left)Band structure of GaAs near the center of the Brillouin zone [16]:s conduction band; HH: heavy hole band; LH: light hole band; SO: split-off band.(Right)Fermi Dirac distribution function for intrinsic semiconductors

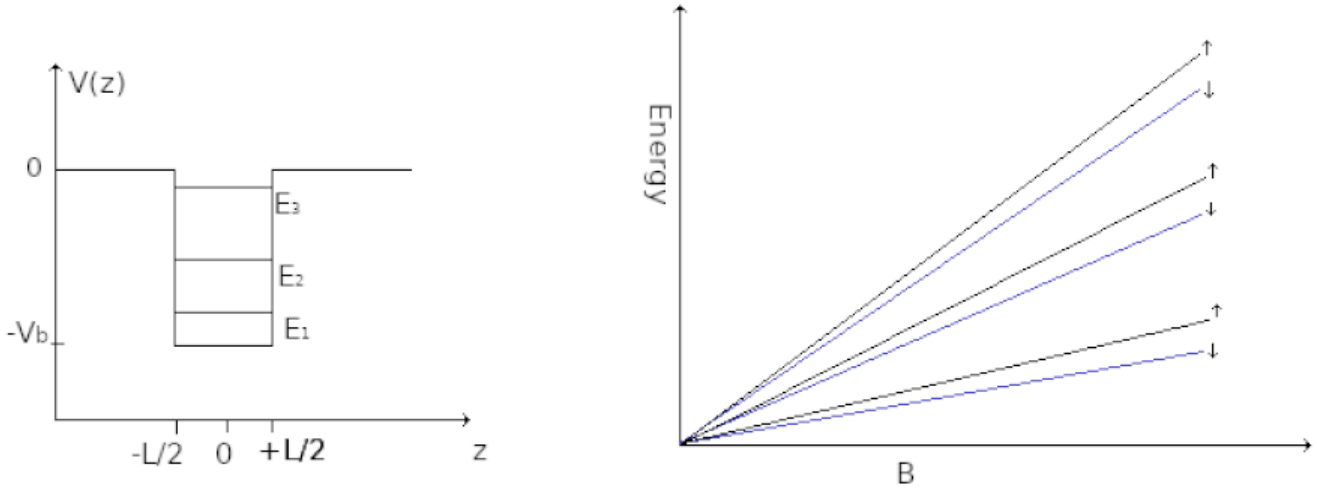

FIG. 4: (Left)Square quantum well[1](Right)Set of Landau levels to a material bulk

It is common to use the so called k.p approximation that describes the energy bands by a Hamiltonian based on the wave-number k and the momentum operator p [17], for simulating the conduction and valence band properties in terms of effective masses. In order to understand this concept we may start with describing the Hamiltonian of the electron in a crystal as [18]

$$H(\mathbf{r}) = \frac{p^2}{2m_0} + V(\mathbf{r}), \tag{1}$$

where $V(\mathbf{r})$ as a periodic potential that responds to the crystal order of the material, and m_0 the free electron mass. The crystalline structure allows defining the particular Bravais lattice of each case, so in this form $U(r) = U(r + R)$ with R a vector of the Bravais lattice. Given this spatial symmetry, Bloch's theorem allows us to define the eigenfunctions (also called Bloch functions) of the electron as follows

$$\psi_{n,k}(\mathbf{r}) = e^{i\mathbf{k}\cdot\mathbf{r}} u_{n,k}(\mathbf{r}), \tag{2}$$

with

$$u_{n,k}(\mathbf{r}) = u_{n,k}(\mathbf{r} + \mathbf{R}). \tag{3}$$

where the number n represents the band index. By applying the eigenfunctions (2) to

the Hamiltonian (1) of a certain crystal, the corresponding band scheme is obtained [19]

$$\left[\frac{p^2}{2m_0} + \frac{\hbar}{m_0}\mathbf{k}\cdot\mathbf{p} + V(\mathbf{r})\right] u_{k,n}(\mathbf{r}) = \left[E_n(\mathbf{k}) - \frac{\hbar^2}{2m_0}\right] u_{n,k}(\mathbf{r}) \tag{4}$$

yielding the n-th band energy $E_n(\mathbf{k})$ with

$$H_0 u_{n,0}(\mathbf{r}) = E_n(0) u_{n,0}(\mathbf{r}) \tag{5}$$

and

$$\left[H_0 + \frac{\hbar}{m_0}\mathbf{k}\cdot\mathbf{p}\right] u_{k,n}(\mathbf{r}) = \left[E_n(\mathbf{k}) - \frac{\hbar^2}{2m_0}\right] u_{n,k}(\mathbf{r}) \tag{6}$$

For values close to $k = 0$, we can use the second-order perturbation theory [20], and assuming that the energy level is not degenerate, then $E_n(\mathbf{k})$ can be expressed as follows

$$u_{n,k}(\mathbf{r}) = u_{n,0}(\mathbf{r}) + \frac{\hbar}{m_0}\sum_{n'\neq n}\frac{\langle u_{n',0}|\mathbf{k}\cdot\mathbf{p}|u_{n,0}\rangle}{E_{n,0} - E_{n',0}}, \tag{7}$$

and

$$E_n(k) = E_n(0) + \frac{\hbar^2 k^2}{2m_0} + \frac{\hbar^2}{m_0}\sum_{n'\neq n}\frac{|\langle u_{n',0}|\mathbf{k}\cdot\mathbf{p}|u_{n,0}\rangle|^2}{E_{n,0} - E_{n',0}}, \tag{8}$$

This expression can be condensed introducing the concept of effective mass m^*,

$$\frac{1}{m^*} = \frac{1}{m_0} + \frac{2}{m_0^2 k^2}\sum_{n'\neq n}\frac{|\langle u_{n',0}|\mathbf{k}\cdot\mathbf{p}|u_{n,0}\rangle|^2}{E_{n,0} - E_{n',0}} \tag{9}$$

in the following way

$$E_n(k) = E_n(0) + \frac{\hbar^2 k^2}{2m^*}. \tag{10}$$

The schematic representation of these bands has been included in Fig.3 (left). At low temperatures semiconductors have a full valence band separated by an energy gap from an empty conduction band. If we assume that the electrons are thermalized, they would follow a Fermi-Dirac distribution as represented in Fig.3 (right).

This seemingly simple model for describing the energy bands can be extended to

heterostructures consisting in a sequence of lattice matched semiconductors, as represented in Fig. 4 (Left). The band profile in this case corresponds to a semiconductor quantum well where the quantum confinement along z-direction leads to the formation of energy levels [1]. The effects of external fields can also be included within the parabolic and k.p approximations. Thus is the case of a uniform magnetic field along the quantization direction z that leads to the formation of Landau levels [21] as displayed in Fig. 4 (Right).

B. Excitons

In the realm of condensed matter physics, the concept of an exciton plays a pivotal role in understanding the behavior of electrons and holes in semiconductors and organic materials. Excitons are fascinating entities, representing a quantum coupling of two fundamental particles: an electron that has gained sufficient energy to traverse the energy gap between the valence and conduction bands, and the hole it leaves behind, which carries an opposite charge. Broadly speaking, excitons come in two principal varieties: Wannier-Mott excitons, often referred to as free excitons, and Frenkel excitons, known as bound excitons. Each type possesses distinctive characteristics that hinge on their environment and spatial scale.

Wannier-Mott excitons predominantly emerge in semiconductors, and they exhibit a size that encompasses several atoms. In contrast, Frenkel excitons are commonly found in organic materials, and they manifest as tightly bound [22] quasiparticles with a much smaller spatial extent, often comparable to the unit cell of the material. In essence, an exciton is a quasiparticle birthed from the electrostatic attraction between an electron and a hole, coaxed into existence by the Coulomb interaction.

The binding energy of an exciton is typically a fraction of the band gap[23], and as a first approximation, it can be considered independent of the particle's spin. This characteristic simplifies our discussion, as we can primarily focus on properties dictated by the orientation of the spins. Thus, in what follows the binding energy will simply be

neglected, and so any Coulomb electron-hole coupling unless those where the exchange interaction plays a role.

However, when delving into the dynamics of excitons, we encounter the intriguing phenomenon of spin relaxation. Spin relaxation occurs when the spin of an exciton interacts with various factors, including external magnetic fields and exchange interactions. The influence of a magnetic field on the spin of excitons is mediated through the Zeeman effect, which refers to the splitting of energy levels within a particle due to its interaction with a magnetic field. In the context of excitons, the Zeeman effect can induce a realignment of the exciton's spin relative to the strength and orientation of the applied magnetic field.

Additionally, exchange interactions come into play, a class of interactions governing the correlation between the spins of two particles. For excitons, exchange interactions lead to correlated spins between the constituent electron and hole, thereby influencing the overall spin properties of the exciton. Thus, while the binding energy may remain relatively constant, the spin orientation of excitons can undergo dynamic changes, offering a rich field of study with implications for various applications in condensed matter physics.

C. Optical selection rules and circularly polarized light.

The possible transitions and the number of those that actually happen are not the same, in general some transitions have such a low probability of occurrence that they are considered prohibited. On the contrary some of these transitions are so likely that they occur and they are called allowed transitions. The rules for choosing which transitions are allowed are called selection rules. According to the basic time-resolved perturbation approach in quantum mechanics, the transition probability per unit time can be calculated using the Fermi Golden Rule [1]

$$P_{v,c} = \frac{2\pi}{\hbar}|\langle\psi_{c,k}|V|\psi_{v,k}\rangle|^2\delta\left(E_c - E_v - \hbar\omega\right) \tag{11}$$

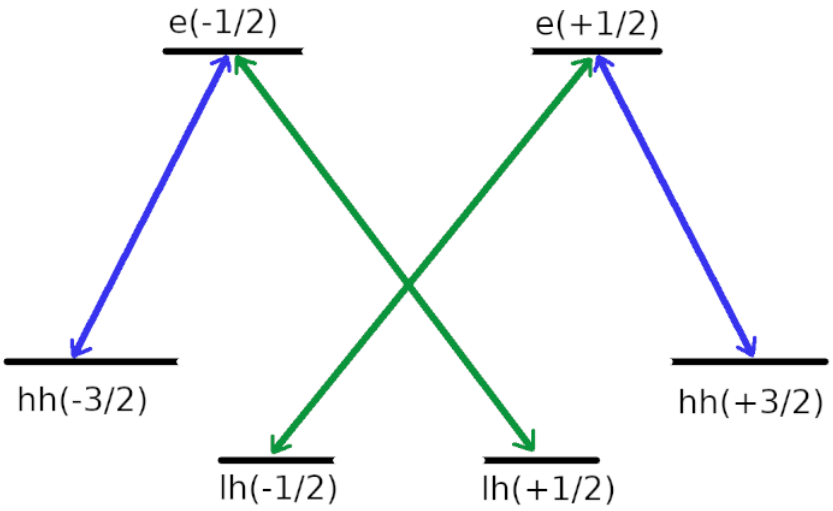

FIG. 5: transitions between levels with j = 3/2 and j = 1/2 and the levels with j = 1/2 ,absorption of a right-polarized photon [18]

between the valence band state $-E_v$ and the conduction band state, E_c emitting a photon with energy $\hbar\omega$. Given the electron photon interaction term $V = \frac{ieF}{2m_0\omega}\epsilon\mathbf{p}$, where F is the wave electric field with polarization ϵ, the selection rules for the optical transitions are determined by the matrix element

$$\langle\psi_{c,k}|V|\psi_{v,k}\rangle \propto \int \psi_v^*\epsilon\mathbf{p}\psi_c \, \mathrm{d}^3r, \tag{12}$$

where ψ_1^* and ψ_2 are the wave functions of the initial and final states, and $\mathbf{p}$ is the momentum operator. The transition probability is proportional to the square of this integral, so, if the result is zero then we called that transition forbidden.

To describe the selection rules in semiconductors it is necessary to fulfill the conservation of angular momentum and energy. Circularly polarized photons can be left or right polarized, and thus their momentum can be projected to have values of +1, -1, in fundamental units, h. When absorbing or emitting a circularly polarized photon, its angular momentum is shared with the electron-hole pair, depending on the momentum of the electron, and the hole and the shape of the particular band structure of

the crystal. Some of the allowed transitions for the absorption of a photon with right circular polarization have been represented in Fig. 5 and will be used later.

In the case of semiconductors such as InGaAs, the selection rules are influenced by the band structure of the material and the conservation of angular momentum. The total angular momentum of the exciton must be conserved during the optical transition. This implies that the change in angular momentum of the electron and hole, together with the angular momentum of electromagnetic radiation, must cancel out.

The energy of the photon absorbed or emitted during the transition must match the energy difference between the energy levels of the electron and the hole involved in the transition. This is because the energy of a photon is proportional to its frequency, and the energy of an electron or a hole is determined by the energy of its band, and whether these energies are sufficient to allow a transition, as described by Eq. 11. For illustration, if an electron is excited from the valence band to the conduction band, it will absorb a photon with an energy equal to the difference between the two bands, which is embedded within the delta function of that equation. The backward process can also plausible, in which a photon is emitted when an electron recombines from the conduction band to the valence band.

In general, the optical behavior of materials is strongly related to their electronic structure, in such a way that the conservation of energy and momentum when determining the optical transitions of semiconductors can explain phenomena such as reflection, refraction and scattering of light from the materials.

D. Hamiltonian exciton in a quantum well

In our case we study confined electron-hole pairs, in the presence of an external magnetic field. In order to model its electronic structure we use the parabolic effective mass approximation described earlier where the Hamiltonian for either an electron or a hole is given by

$$H = T + V + H_{Zeeman} + H_{Landau} \tag{13}$$

Where T is the kinetic energy operator of the electron, V is the potential energy operator due to the confinement in the quantum well, H_{Zeeman} is the Zeeman energy due to the interaction of the magnetic field with the electronic spin, and the Landau quantization energy due to the interaction of the magnetic field with the electron motion is produced by H_{Landau}, in the case of quantum wells. Now, the Zeeman energy could be written as

$$H_{Zeeman} = g_s \cdot \mu_B \cdot B \cdot S \tag{14}$$

with g_s, the effective g-factor, μ_B is the Bohr magneton, B is the magnetic field strength, and S the spin. The Landau quantization energy levels represented in Fig. 4 (right), is defines as [1]

$$H_{Landau} = \hbar \cdot \omega_c \cdot \left(N + \frac{1}{2}\right) \tag{15}$$

Where $\omega_c = \frac{eB}{m^* c}$ is the cyclotron frequency with $N = 0, 1, 2...$, a positive integer called the Landau level index. So, the energy for an electron (hole) confined in a quantum well in the presence of a magnetic field could be expressed as

$$\begin{aligned} E_{N,s} &= \frac{\hbar e B}{m^* c}\left(N + \frac{1}{2}\right) + \frac{s}{2} \cdot g\mu_B B \\ s &= \pm 1 \end{aligned} \tag{16}$$

E. Density of states 2D

In order to describe how electrons occupy the available energy levels it is sometimes possible to assume that they are thermalized defining a Fermi level conditioned by the amount of free electrons in the material, the effective temperature, and the density of energy states, which determines how many electronic states are in some energy range.

In our case the density of 2D states in the presence of an external magnetic field must take into account the quantization of the electronic energy levels due to the magnetic

field, as well as the spin splitting of the energy levels due to the Zeeman interaction [1]

$$\rho_m(\varepsilon) = \frac{S}{2\pi\lambda^2} \sum_{N,\sigma_z} \delta\left[\varepsilon - \xi_m - \left(N + \frac{1}{2}\right)\hbar\omega_{\rm q} - g^*\mu_{\rm B}B\sigma_z\right]. \tag{17}$$

The variable ε represents the energy of the electronic states, S is the system area, and $\rho_m(\varepsilon)$ is the DOS for the m-th energy level in the quantum well (The first level to our case). The sum over the Landau levels and spin quantum numbers gives the total density of states in the 2D. The variable ξ_m is the energy of the m-th confined state, and the sum over N and σ_z takes into account the quantization of the electronic energy levels due to the magnetic field, while σ_z is the z component of the spin quantum number and takes values of $\pm\frac{1}{2}$. The delta function $\delta\left[\varepsilon - \xi_m - \left(n + \frac{1}{2}\right)\hbar\omega_{\rm q} - g^*\mu_{\rm B}B\sigma_z\right]$ determines the energy value of each electronic state. The magnetic length is given by $\lambda = \sqrt{\frac{\hbar}{eB}}$.

If equilibrium is reached, and the charge carriers attain certain effective temperature, we can assume the spin thermalization in the semiconductor material that distributes the orientation of electronic spins according to their energy position. The tuning of the Fermi level with magnetic field and temperature can be achieved by changing the external magnetic field that modifies these energy levels.

F. Electron-hole exchange interaction

The electron-hole exchange interaction is a property that affects the energy ordering of the exciton states according to the spin of their constituents electrons and holes. This allows resolving bright from dark excitons with optically forbidden transitions [24]. The emergence of interaction exchange occurs as a result of the superposition of the electron and hole wave functions, so when excitons are restricted to smaller volumes, such as in narrow quantum wells Fig. 4 (left) one can expect more intense exchange interaction. For our analysis, that is reduced to the spin dependent components to the energies of electrons and holes, the Hamiltonian of the ground state for the electron-hole pairs can

be reduced to

$$H = g_e \mu_B B \cdot S + g_h \mu_B B \cdot j_z - \frac{2}{3}\delta_0 S_z \cdot j_z \tag{18}$$

where S is the electron spin, $j_z = \pm 3/2$ is the hole spin, and δ_0 quantifies the strength of the exchange interaction, as defined in Ref. [25].

In contrast, if the thermalization process cannot be guaranteed, the spin dynamics can be emulated by using the density matrix method and master equations as described in Ref. [26]. The statistical state of a quantum system can be effectively described through the density matrix formalism and this proves to be particularly beneficial in the case of open quantum systems, where a system interacts with its surroundings [27]. The density matrix noted as ρ, is a matrix that represents the state of a quantum system. It is Hermitian, with a unitarian trace, symmetric and has a 1 sum of its diagonal elements (trace).

The probability distribution of a quantum system can be calculated using the density matrix, which also allows for determining its entropy and energy. Furthermore, the density matrix is a valuable tool for describing the time evolution of a quantum system, and when we need to know how the system interact with the universe then we use the evolution of the density matrix in open quantum systems that follows the Lindblad equation. This is a non-unitary equation to describe the interaction between the system and the environment.

In the case of open quantum systems, the density matrix evolves according to the Lindblad equation. The Lindblad equation is a non-unitary equation that describes the temporal evolution of the density matrix in the presence of interactions with the environment and it has the following general form $d\rho/dt = -i[H, \rho] + \sum (L\rho L^+ - 1/2 \{L^+ L, \rho\})$ where H is the Hamiltonian operator of the system, L are the Lindblad operators that represent the interaction with the environment, and $[\hat{\rho}, \hat{H}]$denotes the anticommutator of $\hat{\rho}$ and $\hat{H}$.

$$i\hbar \frac{\partial \hat{\rho}}{\partial t} = -[\hat{\rho}, \hat{H}] = -(\hat{\rho}\hat{H} - \hat{H}\hat{\rho}) \tag{19}$$

First, the density matrix is defined in terms of the matrix elements. The notation ρ_{mn} means the element at position (m, n) of the matrix. The expression $\rho_{mn} = \langle m|\rho|n\rangle$ is used, which represents the expected value of between the states $|m\rangle$ and $|n$. The operator ρ is defined as $|j\rangle\langle j|$, which means that ρ is the projector of the state $|j\rangle$. A pure state is a state in which the system is definitely in a single state, and the density matrix is simply a projection operator onto that state.

Now we can define the expectation value of an observable $\langle\hat{O}\rangle$ as the average value of the observable, and it is calculated by taking a weighted average of the eigenvalues of the observable, [28] with the weights being the probabilities of the system being in each of the possible states

$$\frac{d\rho_{mn}}{dt} = -\frac{i}{\hbar}\left(\langle m|\hat{H}\rho|n\rangle - \langle m|\hat{\rho}\hat{H}|n\rangle\right). \tag{20}$$

Now we rewrite the density matrix in terms of its matrix elements using the completeness relation $\sum_j |j\rangle\langle j| = 1$ The completeness relation states that any state in the system can be expressed as a superposition of the basis states of the system and we can rewrite the equation of motion as follows

$$\frac{d\rho_{mn}}{dt} = -\frac{i}{\hbar}\sum_j\left(\langle m|\hat{H}|j\rangle\langle j|\rho|n\rangle - \langle m|\rho|j\rangle\langle j|\hat{H}|m\rangle\right) \tag{21}$$

This equation of motion is expressed in terms of the matrix elements of the Hamiltonian H_{mj} , and the density matrix, ρ_{mn},

$$\frac{d\rho_{mn}}{dt} = -\frac{i}{\hbar}\sum_j\left(H_{mj}\rho_{jn} - H_{jm}\rho_{mj}\right). \tag{22}$$

Now we want to apply such a description to the characterization of the dynamics of exciton ground states in the presence of a magnetic field. The excitonic basis states in this case are the eigenstates of the total angular momentum operator J_z and the spin operator S_z. We use the J_z operator as the component of the angular momentum

operator along the z-axis that in the matrix representation the operator for heavy holes can be written as

$$J_z = \begin{pmatrix} 3/2 & 0 \\ 0 & -3/2 \end{pmatrix}.$$

Then, the excitonic basis states are defined as the eigenstates of the total angular momentum operator $J_z + Sz$, where Sz is the component of the electron spin operator along the z-axis. With $|J_z + Sz\rangle \langle J_z + Sz|$, a projection operator onto the excitonic basis state$|J_z + Sz\rangle$.

The following lines show how these projection operators apply to heavy hole and electron states in different spin and angular momentum configurations, as follows: $|J_z\rangle |Sz\rangle \langle Sz| \langle Jz|$ then , first for dark $|3/2\rangle|1/2\rangle\langle 1/2|\langle 3/2| = |2\rangle\langle 2|$ indicates how a specific state is projected into the space of excitonic ground states. For example, in this case, the result is the projection in the excitonic state with a total angular momentum of 2. And for the other cases bright $|3/2\rangle |-1/2\rangle \langle -1/2|\langle 3|2| =| 1\rangle\langle 1|$, bright $|-3/2\rangle|1/2\rangle\langle 1/2|\langle -3/2| = |-1\rangle\langle -1|$, dark $|-3/2\rangle$ $|-1/2\rangle\langle -1/2|\langle -3/2| = |-2\rangle\langle -2|$.

Thus, making use of a matrix notation for the electron spin states, up and down, defined as $|1/2\rangle = \begin{pmatrix} 1 \\ 0 \end{pmatrix}$;$|-1/2\rangle = \begin{pmatrix} 0 \\ 1 \end{pmatrix}$ and using the Pauli matrices to represent the spin of electrons and holes

$$\sigma_x = \begin{pmatrix} 0 & 1 \\ 1 & 0 \end{pmatrix} \quad \sigma_y = \begin{pmatrix} 0 & -i \\ i & 0 \end{pmatrix} \quad \sigma_z = \begin{pmatrix} 1 & 0 \\ 0 & -1 \end{pmatrix} \tag{23}$$

we can get the expectation values of the Pauli matrices for the spin states 1/2,1/2 and 1/2,1/2 such as

$$\begin{aligned} &\langle -1/2\,|\sigma_x|\,1/2\rangle = 1 \quad \langle -1/2\,|\sigma_y|\,1/2\rangle = i \quad\;\; \langle 1/2\,|\sigma_z|\,1/2\rangle = 1 \\ &\langle 1/2\,|\sigma_x|\,-1/2\rangle = 1 \;\; \langle 1/2\,|\sigma_y|\,-1/2\rangle = -i \;\; \langle 1/2\,|\sigma_z|\,-1/2\rangle\rangle = -1 \end{aligned} \tag{24}$$

The expected value of the spin density will not be zero when the state of the electron

is a superposition of spin states. So we can now calculate their value along each direction, as $\langle S_i \rangle \equiv \left\langle \frac{\sigma_j}{2} \right\rangle$ then in x direction we get $\langle S_x \rangle \equiv \left\langle \frac{\sigma_x}{2} \right\rangle$

$$\begin{aligned}
\left\langle \frac{\sigma_x}{2} \right\rangle = \frac{1}{2}\Bigg(& \rho_{22} \langle 2|\sigma_x|2\rangle + \rho_{21} \langle 1|\sigma_x|2\rangle \\
& + \rho_{2-1} \langle -1|\sigma_x|2\rangle + \rho_{2-2} \langle -2|\sigma_x|2\rangle + \rho_{12} \langle 2|\sigma_x|1\rangle \\
& + \rho_{11} \langle 1|\sigma_x|1\rangle + \rho_{1-1} \langle -1|\sigma_x|1\rangle + \rho_{1-2} \langle -2|\sigma_x|1\rangle \Bigg) \\
& + \frac{1}{2}\Bigg(\rho_{-12} \langle 2|\sigma_x| - 1\rangle + \rho_{-11} \langle 1|\sigma_x| - 1\rangle \\
& + \rho_{-1-1} \langle -1|\sigma_x| - 1\rangle + \rho_{-1-2} \langle -2|\sigma_x| - 1\rangle \\
& + \rho_{-22} \langle 2|\sigma_x| - 2\rangle + \rho_{-21} \langle 1|\sigma_x| - 2\rangle \\
& + \rho_{-2-1} \langle -1|\sigma_x| - 2\rangle + \rho_{-2-2} \langle -2|\sigma_x| - 2\rangle \Bigg)
\end{aligned} \tag{25}$$

To see the terms in a explicit way in the exitonic basis we have

$$\begin{aligned}
\rho_{-2-1} \langle -1 \left|\sigma_x\right| - 2\rangle &= \rho_{-2-1} \left\langle -\frac{3}{2} \left| \left\langle \frac{1}{2} \left|\sigma_x\right| -\frac{1}{2} \right\rangle \right| -\frac{3}{2} \right\rangle = \rho_{-2-1} \\
\rho_{-1-2} \langle -2 \left|\sigma_x\right| - 1\rangle &= \rho_{-1-2} \left\langle -\frac{3}{2} \left| \left\langle -\frac{1}{2} \left|\sigma_x\right| \frac{1}{2} \right\rangle \right| -\frac{3}{2} \right\rangle = \rho_{-1-2} \\
\rho_{21} \langle 1 \left|\sigma_x\right| 2\rangle &= \rho_{21} \left\langle \frac{3}{2} \left| \left\langle -\frac{1}{2} \left|\sigma_x\right| \frac{1}{2} \right\rangle \right| \frac{3}{2} \right\rangle = \rho_{21} \\
\rho_{12} \langle 2 \left|\sigma_x\right| 1\rangle &= \rho_{12} \left\langle \frac{3}{2} \left| \left\langle \frac{1}{2} \left|\sigma_x\right| -\frac{1}{2} \right\rangle \right| \frac{3}{2} \right\rangle = \rho_{12}.
\end{aligned} \tag{26}$$

Then, removing the null terms, the expected value can be reduced to very compact expressions

$$\langle S_x \rangle = \frac{1}{2} \left(\rho_{12} + \rho_{21} + \rho_{-1-2} + \rho_{-2-1} \right) \tag{27}$$

An analogous procedure can be performed with the expected value of J_z. In this case we have

$$\langle J_z \rangle = \sum_m \langle m|\rho|n\rangle \langle n \left|J_z\right| m\rangle. \tag{28}$$

In this case, the non zero values of the matrix elements in the excitonic basis are

$$\begin{aligned}
\rho_{11}\langle 1\,|J_z|\,1\rangle &= \rho_{11}\left\langle -\frac{1}{2}\left|\left\langle \frac{3}{2}\,|J_z|\,\frac{3}{2}\right\rangle\right|-\frac{1}{2}\right\rangle = \frac{3}{2}\rho_{11}\\
\rho_{22}\langle 2\,|J_z|\,2\rangle &= \rho_{22}\left\langle \frac{1}{2}\left|\left\langle \frac{3}{2}\,|J_z|\,\frac{3}{2}\right\rangle\right|\frac{1}{2}\right\rangle = \frac{3}{2}\rho_{22}\\
\rho_{-1-1}\langle -1\,|J_z|\,-1\rangle &= \rho_{-1-1}\left\langle \frac{1}{2}\left|\left\langle -\frac{3}{2}\,|J_z|\,-\frac{3}{2}\right\rangle\right|\frac{1}{2}\right\rangle = -\rho_{-1-1}\frac{3}{2}\\
\rho_{-2-2}\langle -2\,|J_z|\,-2\rangle &= \rho_{-2-2}\left\langle -\frac{1}{2}\left|\left\langle -\frac{3}{2}\,|J_z|\,-\frac{3}{2}\right\rangle\right|-\frac{1}{2}\right\rangle = -\frac{3}{2}\rho_{-2-2}
\end{aligned} \tag{29}$$

with reduce the expected value for J_z to

$$\langle J_z\rangle = \frac{3}{2}\left(-\rho_{11}+\rho_{22}+\rho_{-1-1}-\rho_{-2-2}\right) \tag{30}$$

Beside the average value of each component of the spin operators, we must consider the exchange terms that characterize the correlation between the hole and electron spin, which are proportional to the operator $\vec{Q} = 2/3Jz\vec{S}$ [26]. Thus, in an analogous way for Q_x, we can set

$$\begin{aligned}
\langle Q_x\rangle = \langle\frac{2}{3}J_zS_x\rangle &= \frac{1}{2}\cdot\frac{2}{3}\left(\frac{3}{2}\rho_{12}+\frac{3}{2}\rho_{21}-\frac{3}{2}\rho_{-1-2}-\frac{3}{2}\rho_{-2-1}\right)\\
&= \frac{1}{2}\left(\rho_{12}+\rho_{21}-\rho_{-1-2}-\rho_{-2-1}\right)
\end{aligned} \tag{31}$$

and also for the expected value Q_z

$$\begin{aligned}
\langle Q_z\rangle = \left\langle\frac{2}{3}J_zS_z\right\rangle &= \frac{2}{3}\left(-\frac{3}{2}\cdot\frac{1}{2}\rho_{11}-\frac{3}{2}\cdot\frac{1}{2}\rho_{-1-1}+\frac{3}{2}\cdot\frac{1}{2}\rho_{22}+\frac{3}{2}\cdot\frac{1}{2}\rho_{-2-2}\right)\\
&= \frac{1}{2}\left(-\rho_{11}-\rho_{-1-1}+\rho_{22}+\rho_{-2-2}\right)
\end{aligned} \tag{32}$$

Also the expected values for Q_y, S_y, S_z can be expressed in terms of components of the density matrix ρ_{ij} as follows

$$\langle Q_y\rangle = \frac{2}{3}\left(\frac{1}{2}\frac{3}{2}i\rho_{21}-\frac{3}{2}\frac{1}{2}i\rho_{12}-\frac{3}{2}\frac{1}{2}i\rho_{-1-2}+\frac{3}{2}\frac{1}{2}i\rho_{-2-1}\right) = \frac{i}{2}\left(\rho_{21}-\rho_{12}-\rho_{-1-2}+\rho_{-2-1}\right). \tag{33}$$

Likewise,

$$\langle S_y \rangle = \frac{i}{2} \left(\rho_{21} - \rho_{12} + \rho_{-1-2} - \rho_{-2-1} \right) \tag{34}$$

and

$$\langle S_z \rangle = \frac{1}{2} \left(\rho_{22} - \rho_{11} + \rho_{-1-1} - \rho_{-2-2} \right), \tag{35}$$

In what follows we will follow the paths indicated in Ref. [26] that provides a theoretical framework for understanding the spin dynamics of excitons in quantum wells and open all the algebraic steps. That reference shows that the spin dynamics is dominated by the single-particle hole spin-flip mechanism and also that the two-dimensional confinement and low temperatures are the most important factors that stabilize the hole spin orientation within the exciton.

The first step is to correlate the dynamics of the spin related operators with our experimental observables, the intensities of circularly polarized exciton emissions: $I^+ \propto \rho_{11}$ and $I^- \propto \rho_{-1-1}$. We can thus define the number of bright excitons (those emitting light) as $N_b = \rho_{11} + \rho_{-1-1}$ while the dark ones would correspond to $N_d = \rho_{22} + \rho_{-2-2}$, and prove that

$$I^+ = \frac{N_b}{2} + \frac{1}{2}\left(\frac{J_z}{3} - S_z \right) = \frac{1}{2}\left[\left(\frac{1}{2} - Q_z \right) + \frac{1}{3} J_z - S_z \right]. \tag{36}$$

By substituting the expressions of the mean values of S_z, J_z, Q_z we get

$$\begin{aligned} I^+ = \frac{1}{2}\Big[& \frac{1}{2} - \frac{1}{2}\left(-\rho_{11} - \rho_{-1-1} + \rho_{22} + \rho_{-2-2} \right) \\ & + \frac{1}{2}\left(\rho_{11} - \rho_{-1-1} + \rho_{22} - \rho_{-2-2} \right) \\ & - \frac{1}{2}\left(-\rho_{11} + \rho_{-1-1} + \rho_{22} - \rho_{-2-2} \right) \Big] = \rho_{11}. \end{aligned} \tag{37}$$

In turn, in the case of I^- we can prove that

$$I^- = \frac{1}{2}\left[\left(\frac{1}{2} - Q_z \right) - \left(\frac{1}{3} J_z - S_z \right) \right] \tag{38}$$

by substituting the expressions of S_z, J_z, Q_z in I^-. This yields

$$\begin{aligned} I^- = \frac{1}{2}\Bigg[\frac{1}{2} - \frac{1}{2}\Big(-\rho_{11} - \rho_{-1-1} + \rho_{22} + \rho_{-2-2}\Big) \\ - \Bigg(\frac{1}{2}\Big(\rho_{11} - \rho_{-1-1} + \rho_{22} - \rho_{-2-2}\Big) \\ - \frac{1}{2}\Big(-\rho_{11} + \rho_{-1-1} + \rho_{22} - \rho_{-2-2}\Big)\Bigg)\Bigg] = \rho_{-1-1}. \end{aligned} \tag{39}$$

Note that, given the normalization $\sum_j \rho_{jj} = 1$, then $N_b + N_d = 1$, in this case. Additionally, according to Eq. 32, $Q_z = 1/2(Nd - N_b) = 1/2 - N_b$.

Then the degree of circular polarization, defined as [11]

$$P = \frac{I^+ - I^-}{I^+ + I^-} \tag{40}$$

results in

$$P = \frac{\frac{1}{3}J_z - S_z}{\frac{1}{2} - Q_z} \tag{41}$$

Or expressed in terms of the number of bright exciton N_b

$$\Rightarrow P = \frac{I^+ - I^-}{I^+ + I^-} = \frac{\rho_{11} - \rho_{-1-1}}{\rho_{11} + \rho_{-1-1}} = \frac{\frac{J_z}{3} - S_z}{Nb} \tag{42}$$

Now lets assume the excitons confined and consider just the two spin-split ground states of the conduction band present, $S_z = \pm\frac{1}{2}$, and two in the valence band, corresponding to the heavy hole sub-band with total angular momentum $J = \pm\frac{3}{2}$. The states of the heavy hole exciton are described by the basis $|J_z + S_z\rangle$ Thus, the simplest Hamiltonian for the spin of the heavy hole exciton in a magnetic field is given by Eq. 18. We will further neglect the effect of the hole Zeeman splitting and define $\hbar\vec{\omega} = g\mu_B\vec{B}$. Then, since the equation of motion of any observable $\hat{O}$ is

$$\frac{d\hat{O}}{dt} = \frac{1}{i\hbar}[\hat{O}, \hat{H}]. \tag{43}$$

This equation includes just coherent terms, responsible for the reversible and deterministic dynamics of the quantum system.

The dynamics of the spin $\vec{S}$ in the presence of the magnetic field and the exchange term is given by

$$\frac{d\vec{S}}{dt} = -\frac{i}{\hbar}\left[\vec{S}(\hbar\vec{\omega}\vec{S}) - (\hbar\vec{\omega}\vec{S})\vec{S} - \frac{2}{3}\delta\left(\vec{s}J_zS_z - J_zS_z\vec{S}\right)\right]$$

Now, using Dyakonov's definition of $\tilde{\delta} = \frac{\delta}{\hbar}$, [26] and taking a vector $\hat{n} = (0, 0, 1)$ normal to the confinement direction, one has

$$\frac{d\vec{s}}{dt} = -i\left[\vec{s}(\vec{\omega}\vec{s}) - (\vec{\omega}\vec{s})\vec{s} - \frac{2}{3}\tilde{\delta}\left(\vec{s}J_z(\vec{s}\cdot\hat{n}) - J_z(\vec{s}\hat{n})\vec{s}\right)\right] \tag{44}$$

We must introduce now the Levi-Civita symbol ε_{jik} to represent the cross product. This symbol is 1 if (i, j, k) is one of the cyclic permutations, -1 if it is one of the anti cyclic permutations, and 0 otherwise i.e.

$$\varepsilon_{ijk} = \begin{cases} 1 \text{ if } (i,j,k) \text{ then } (1,2,3),(2,3,1),(3,1,2) \\ -1 \text{ if } (i,j,k) \text{ then } (3,2,1),(1,3,2),(2,1,3) \\ 0 \text{ else } i=j, j=k, k=i \end{cases}. \tag{45}$$

This condenses the vector cross product $\vec{a} \times \vec{b} = \vec{c}$

$$c_i = \sum_{j,k=1}^{3} \varepsilon_{ijk} a_j b_k \tag{46}$$

in such a way that the terms in Eq. 44 can be written as follows with $\vec{s}$ factored from both parts of the expression. We thus obtain

$$\vec{s}(\vec{\omega}\vec{s}) - (\vec{\omega}\vec{s})\vec{s} = \vec{s}\left(\sum_{i=1}^{3}\omega_i s_i\right) - \left(\sum_{i=1}^{3}\omega_i s_i\right)\vec{s} \tag{47}$$

$$= \sum_{j=1}^{3} \hat{n}_j S_i \sum_{i=1}^{3} \omega_i S_i - \sum_{i=1}^{3} \omega_i S_i \sum_{j=1}^{3} \hat{n}_j S_j = \sum_{j=1}^{3} \sum_{i=1}^{3} \hat{n}_j \omega_i \left[S_j S_i - S_i S_j \right] \tag{48}$$

This expression is simplified in terms of the Levi-Civita symbol, resulting in

$$\vec{s}(\vec{\omega}\vec{s}) - (\vec{\omega}\vec{s})\vec{s} = -\sum_{i=1}^{3} \sum_{j=1}^{3} \sum_{k=1}^{3} \hat{n}_i \omega_j \varepsilon_{jik} S_k = i\vec{\omega} \times \vec{s}. \tag{49}$$

Therefore, with this development we show how the initial expression that involves scalar and cross products is simplified and we arrive at the final equation that describes the evolution of the spin $\vec{s}$ under the influence of $\vec{\omega}$, $\tilde{\delta}$ and J_z in a compact form

$$\frac{d\vec{s}}{dt} = \vec{\omega} \times \vec{s} - \frac{2}{3} \tilde{\delta} \hat{n} \times J_z \vec{s} \tag{50}$$

We should note that the operator J_z is a constant of motion, meaning that its derivative with respect to time is zero i.e. $\frac{dJ_z}{dt} = 0$. This is because $[J_z, \hat{H}] = 0$, which implies that J_z is a conserved operator in the system. Analogously, we obtain the equation that describes the evolution of $J_z\vec{S}$ as a function of $\vec{\omega}$, J_z, $\vec{S}$ and the term of exchange as

$$\frac{d\left(J_z \vec{S}\right)}{dt} = \vec{w} \times \left(J_z \vec{S}\right) - \frac{2}{3} \delta \hat{n} \times J_z^2 \vec{S} \tag{51}$$

Now we rewrite the expression to describe how the spin vector $\vec{S}$ changes with time. It includes two terms, $\vec{\omega} \times \vec{S}$ representing the spin precession around the magnetic field, $\vec{\omega}$ and $-\tilde{\delta}\hat{n}_3 \times \vec{Q}$ representing the influence of the exchange term $\tilde{\delta}$ and a vector $\hat{n}_3$ pointing in the z direction, so that

$$\frac{d\vec{S}}{dt} = \vec{\omega} \times \vec{S} - \tilde{\delta} \hat{n}_3 \times \vec{Q} \quad \text{with} \quad n_3 = (0, 0, 1) \tag{52}$$

The expression in Eq. 51 transforms into

$$\frac{d\vec{Q}}{dt} = \vec{\omega} \times \vec{Q} - \tilde{\delta} n_3 \times \vec{S} \tag{53}$$

Here, the term, $\vec{\omega}\times\vec{Q}$ represents the precession of $\vec{Q}$ around the magnetic field, $\vec{\omega}$, while $-\tilde{\delta}n_3\times\vec{S}$ represents the interaction between $\vec{S}$ and $\vec{Q}$ due to the exchange contribution $\tilde{\delta}$ and the vector $\hat{n}_3$.

The vector products are given by

$$\vec{\omega}\times\vec{S}=\begin{vmatrix}\hat{i} & \hat{j} & \hat{k}\\ \omega_x & \omega_y & \omega_z\\ S_x & S_y & S_z\end{vmatrix}=\hat{i}\left(\omega_y S_z-\omega_z S_y\right)-\hat{j}\left(\omega_x S_z-\omega_z S_x\right)+\hat{k}\left(\omega_x S_z-\omega_z S_x\right) \tag{54}$$

and

$$\hat{n}_3\times\vec{S}=-\hat{i}\left(S_y\right)+\hat{j}\left(S_x\right). \tag{55}$$

So, we can decompose Eq. 53 as

$$\begin{aligned}\frac{dQ_z}{dt}&=\omega_x Q_y-\omega_y Q_x\\ \frac{dQ_y}{dt}&=-\omega_x Q_z+\omega_z Q_x-\tilde{\delta}S_x\\ \frac{dQ_x}{dt}&=\omega_y Q_z-\omega_z Q_y+\tilde{\delta}S_y\end{aligned} \tag{56}$$

and the following equations for the components of the vector $\vec{S}$,

$$\begin{aligned}\frac{dS_z}{dt}&=\omega_x S_y-\omega_y S_x\\ \frac{dS_y}{dt}&=-\omega_x S_z+\omega_z S_x-\tilde{\delta}Q_x\\ \frac{dS_z}{dt}&=\omega_y-\omega_z S_y+\tilde{\delta}Q_y\end{aligned} \tag{57}$$

This, will deliver the evolution of the vector $\vec{Q}$ by describing how its components change in time due to precession around the magnetic field and the interaction with the spin vector $\vec{S}$. Furthermore, it is established how the components of $\vec{S}$ change in response to the aforementioned influences. These equations are fundamental to understand the dynamics of exciton spins subjected to a magnetic field.

V. INCOHERENT PROCESSES

The dynamic equations described thus far included just coherent terms. The incoherent terms are associated with processes, such as dissipation and decoherence, which introduce irreversibility and cause the system to lose coherence. They model the interactions and energy exchange with the environment which can lead to phenomena such as relaxation (energy dissipation) and dephasing (loss of phase coherence). Understanding these processes is crucial for accurately modeling and predicting the behavior of open quantum systems in practical applications.

The incoherent terms in the Lindblad equation are introduced "by hand" in a phenomenological way because the detailed microscopic dynamics of the system-environment interaction are often complex and challenging to describe precisely. Instead of deriving these terms from first principles, they are added based on general physical principles and experimental observations.

Thus, the time evolution of an operator $\hat{O}$ will be given by

$$\frac{d\hat{O}}{dt} = -\frac{i}{\hbar}[\hat{O}, \hat{H}] + \left.\frac{\partial \hat{O}}{dt}\right|_{\text{incoherent}}. \tag{58}$$

A. Radiative

In order to incorporate recombination processes in the temporal evolution of the components of the density matrix ($\rho_{mm'}$) one may introduce a recombination time, τ_R that will affect components corresponding to optically active states. According to Ref. [26]

$$\left.\frac{\partial \rho_{mm'}}{\partial t}\right|_{\text{inco}} = -\frac{1}{2\tau_R}\left(\delta_{|m|,1} + \delta_{|m'|,1}\right)\rho_{mm'} \tag{59}$$

that has been symmetrized that ensures that the evolution is trace-preserving.

Now we have that the subsequent table of derivatives describe the temporal evolution of the components of the density matrix $\rho_{mm'}$ due to recombination processes present in the Table I

TABLE I: Derivatives of the density $\rho_{mm'}$ with respect to time

Component of $\rho_{mm'}$	**Derivative with respect to time**
ρ_{11}	$-\frac{\rho_{11}}{\tau_R}$
ρ_{-1-1}	$-\frac{\rho_{-1-1}}{\tau_R}$
ρ_{-11}	$-\frac{\rho_{-1}}{\tau_R}$
ρ_{1-1}	$-\frac{\rho_{1-1}}{\tau_R}$
ρ_{12}	$-\frac{\rho_{12}}{2\tau_R}$
ρ_{21}	$-\frac{\rho_{21}}{2\tau_R}$
ρ_{-12}	$-\frac{\rho_{-12}}{2\tau_R}$
ρ_{2-1}	$-\frac{\rho_{2-1}}{2\tau_R}$
ρ_{-12}	$-\frac{\rho_{12}}{2\tau_R}$
ρ_{-1-2}	$-\frac{\rho_{-1-2}}{2\tau_R}$
ρ_{-21}	$-\frac{\rho_{-21}}{2\tau_R}$
ρ_{-2-1}	$\frac{\rho_{-2-1}}{2\tau_R}$

B. Non-Radiative

Analogously, one can describe the rate of change of the diagonal elements ρ_{mm} of the density matrix due to incoherent nonradiative processes

$$\left.\frac{\partial \rho_{mm'}}{\partial t}\right|_{\text{inco}} = -\frac{1}{2\tau_{NR}}\left(\delta_{|m|2} + \delta_{|m'|2}\right)\rho_{mm'}. \tag{60}$$

Here, τ_{NR} represents the nonradiative relaxation time.The term on the right-hand side contains a Kronecker delta functions $\delta_{|m|2}$ and $\delta_{|m'|2}$, which essentially select diagonal elements ($|m| = 2$) of the density matrix. This means it affects elements where m or m' are 2 or -2. The negative sign indicates a decrease in the populations of these diagonal elements due to nonradiative processes.

Some cases of the rate of change for various density matrix elements due to nonradiative processes that can be useful later are presented in the Table II.

TABLE II: Rate of Change of Density Matrix Elements ($\rho_{mm'}$) Due to Non-Radiative Processes

Density Matrix Element	**Rate of Change**	**Relaxation Time**
ρ_{22}	$-\frac{\rho_{22}}{\tau_{NR}}$	τ_{NR}
ρ_{-2-2}	$-\frac{\rho_{-2-2}}{\tau_{NR}}$	τ_{NR}
ρ_{2-2}	$-\frac{\rho_{2-2}}{\tau_{NR}}$	τ_{NR}
ρ_{-22}	$-\frac{\rho_{-22}}{\tau_{NR}}$	τ_{NR}
ρ_{12}	$-\frac{\rho_{12}}{2\tau_{NR}}$	$2\tau_{NR}$
ρ_{21}	$-\frac{\rho_{21}}{2\tau_{NR}}$	$2\tau_{NR}$
ρ_{-12}	$-\frac{\rho_{-12}}{2\tau_{NR}}$	$2\tau_{NR}$
ρ_{2-1}	$-\frac{\rho_{2-1}}{2\tau_{NR}}$	$2\tau_{NR}$
ρ_{-1-2}	$-\frac{\rho_{-1-2}}{2\tau_{NR}}$	$2\tau_{NR}$
ρ_{-2-1}	$\frac{\rho_{-2-1}}{2\tau_{NR}}$	$2\tau_{NR}$
ρ_{1-2}	$-\frac{\rho_{1-2}}{2\tau_{NR}}$	$2\tau_{NR}$
ρ_{-21}	$-\frac{\rho_{-21}}{2\tau_{NR}}$	$2\tau_{NR}$

For total exciton flip processes the relations are analogous, i.e. ρ_{11} to ρ_{-1-1} or ρ_{22} to ρ_{-2-2}. These processes will not change the numbers of N_b and N_d and we will neglect their contribution.

C. Spin Flip

Now we will introduce the temporal evolution of the components of the density matrix due to spin flip processes of either electrons or holes, controlled by the relaxation times τ_e and τ_h, respectively. The following equations show how the different spin components evolve due to spin flip rates as described in Ref. [29]

$$\left.\frac{\partial \rho_{sj,s'j'}}{\partial t}\right|_{sF} = -\frac{1}{\tau_e}\left(\rho_{sj,s'j'} - \frac{1}{2}\delta_{ss'}\sum_{s'}\rho_{s''j,s''j'}\right) - \frac{1}{\tau_h}\left(\rho_{sj,s'j'} - \frac{1}{2}\delta_{jj'}\sum_{j''}\rho_{sj'',s'j'}\right) \tag{61}$$

Table III shows the equations that describes how the spin polarization of the exciton evolves over time.

TABLE III: Derivates with respect to time for spin reversal processes.

Density Matrix Component	**Derivative with respect to time**
ρ_{11}	$-\rho_{11}\left(\frac{1}{2\tau_e}+\frac{1}{2\tau_h}\right)+\frac{\rho_{22}}{2\tau_e}+\frac{\rho_{-2-2}}{2\tau_h}$
ρ_{-1-1}	$-\rho_{-1-1}\left(\frac{1/2\tau_e}{+}\frac{1}{2\tau_h}\right)+\frac{\rho_{-2-2}}{2\tau_e}+\frac{\rho_{22}}{2\tau_h}$
ρ_{22}	$-\rho_{22}\left(\frac{1}{2\tau_e}+\frac{1}{2\tau_h}\right)+\frac{\rho_{11}}{2\tau_e}+\frac{\rho_{-1-1}}{2\tau_h}$
ρ_{-2-2}	$-\rho_{-2-2}\left(\frac{1}{2\tau_e}+\frac{1}{2\tau_h}\right)+\frac{\rho_{-1-1}}{2\tau_e}+\frac{\rho_{11}}{2\tau_h}$
ρ_{12}	$-\frac{\rho_{12}}{\tau_e}-\frac{\rho_{12}}{2\tau_h}+\frac{\rho_{-2-1}}{2\tau_h}$
ρ_{21}	$\frac{\rho_{21}}{\tau_e}-\frac{\rho_{21}}{2\tau_h}+\frac{\rho_{-1-2}}{2\tau_h}$
ρ_{-11}	$-\frac{\rho_{-11}}{\tau_e}-\frac{\rho_{-11}}{\tau_h}$
ρ_{2-2}	$-\frac{\rho_{2-2}}{\tau_e}-\frac{\rho_{2-2}}{\tau_h}$
ρ_{-22}	$-\frac{\rho_{-22}}{\tau_e}-\frac{\rho_{-22}}{\tau_h}$
ρ_{-12}	$-\frac{\rho_{-12}}{\tau_e}+\frac{\rho_{-12}}{2\tau_e}+\frac{\rho_{-21}}{2\tau_e}-\frac{\rho_{-12}}{\tau_h}$
ρ_{2-1}	$-\frac{\rho_{2-1}}{2\tau_e}-\frac{\rho_{2-1}}{\tau_h}+\frac{\rho_{1-2}}{2\tau_e}$
ρ_{-21}	$-\frac{\rho_{-21}}{\tau_e}+\frac{\rho_{-21}}{2\tau_e}+\frac{\rho_{-12}}{2\tau_e}-\frac{\rho_{-21}}{\tau_h}$

D. Photogeneration

Another important interaction with the environment is the creation of electron-hole pairs through photon absorption. These generation terms represent the rates at which density matrix elements associated with different spin states change with time due to photogeneration processes that can be polarization resolved. The values of these terms, which we note as G_{11}, G_{-1-1}, G_{22} and G_{-2-2}, are important for understanding how the exciton polarization evolves in the presence of light pumping

$$\frac{d\rho_{11}}{dt}=G_{11},\frac{d\rho_{-1-1}}{dt}=G_{-1-1},\frac{d\rho_{22}}{dt}=G_{22},\frac{d\rho_{-2-2}}{dt}=G_{-2-2} \tag{62}$$

E. Final Expressions

Then, we now present the expression taking into account the incoherent terms in the change of the component J_z. Incoherent terms are divided into two parts: $\frac{dJ_z}{dt}\Big|_{sf}$ and $\frac{dJ_z}{dt}\Big|$ Recombination $=R+NR$. That is, the radiative and non-radiative part in

a single term.

$$\frac{dJ_z}{dt} = \left.\frac{dJ_z}{dt}\right|_{sf} + \left.\frac{dJ_z}{dt}\right|_{\text{Recombination }=R+NR} \tag{63}$$

That can be written as follows using the detailed terms of the spin flip part

$$\begin{aligned}\frac{dJ_z}{dt} &= \left.\frac{dJ_z}{dt}\right|_{R+NR} + \frac{3}{2}\left(\dot{\rho}_{11}|_{sf} + \dot{\rho}_{22}|_{sf} - \dot{\rho}_{-1-1}|_{sf} - \dot{\rho}_{-2-2}|_{sf}\right) \\ &= \left.\frac{dJ_z}{dt}\right|_{R+NR} + \frac{3}{2}[- \rho_{11}\left(\frac{1}{2\tau_e} + \frac{1}{2\tau_h}\right) + \frac{\rho_{22}}{2\tau_e} + \frac{\rho_{-2-2}}{2\tau_h} - \rho_{22}\left(\frac{1}{2\tau_e} + \frac{1}{2\tau_h}\right) \\ &\quad + \frac{\rho_{11}}{2\tau_e} + \frac{\rho_{-1-1}}{2\tau_h} + \rho_{-1-1}\left(\frac{1}{2\tau_e} + \frac{1}{2\tau_h}\right) - \frac{\rho_{-2-2}}{2\tau_e} - \frac{\rho_{22}}{2\tau_h} \\ &\quad + \rho_{-2-2}\left(\frac{1}{2\tau_e} + \frac{1}{2\tau_h}\right) - \frac{\rho_{-1-1}}{2\tau_e} - \frac{\rho_{11}}{2\tau_h}]\end{aligned} \tag{64}$$

That reduces to the following expression for J_z

$$\frac{dJ_z}{dt} = \left.\frac{dJ_z}{dt}\right|_{R+NR} - \frac{1}{\tau_h}\frac{3}{2}\left(\rho_{11} + \rho_{22} - \rho_{-1-1} - \rho_{-2-2}\right) \tag{65}$$

and finally to

$$\frac{dJ_z}{dt} = \left.\frac{dJ_z}{dt}\right|_{R+NR} - \frac{J_z}{\tau_h} \tag{66}$$

Now, to include the other contributions

$$\begin{aligned}\frac{dJ_z}{dt} &= -\frac{J_z}{\tau_h} + \frac{3}{2}\left(\dot{\rho}_{11}|_{R+NR} + \dot{\rho}_{21}|_{R+NR} - \dot{\rho}_{-1-1}|_{R+NR} - \dot{\rho}_{-2-2}|_{R+NR}\right) \\ &= \frac{-J_z}{\tau_h} - \frac{3}{2\tau_R}\left(\rho_{11} - \rho_{-1-1}\right) - \frac{3}{2\tau_{NR}}\left(\rho_{22} - \rho_{-2-2}\right).\end{aligned} \tag{67}$$

Since $\frac{J_z}{3} - S_z = \rho_{11} - \rho_{-1-1}$ and $\frac{J_z}{3} + S_z = \rho_{22} - \rho_{-2-2}$ we can rewrite the last expression in a more compact representation

$$\frac{dJ_z}{dt} = -\frac{J_z}{\tau_h} - \frac{J_z - 3S_z}{2\tau_R} - \frac{J_z + 3S_z}{2\tau_{NR}} \tag{68}$$

The generation terms can be added now and we get

$$\frac{dJ_z}{dt} = \frac{-J_z}{\tau_h} - \frac{J_z - 3S_z}{2\tau_R} - \frac{J_z + 3S_z}{2\tau_{NR}} + \frac{3}{2}\left[(G_{11} - G_{-1-1}) + (G_{22} - G_{-2-2})\right] \tag{69}$$

In the case of the z-component of the correlation term, we use

$$\frac{dQ_z}{dt} = (\omega_x Q_y - \omega_y Q_x) + \dot{Q}_z\Big|_{sf} + \dot{Q}_z\Big|_{R+NR}. \tag{70}$$

where z and x are the components of the angular frequency of the magnetic field in the z and x directions, respectively and $(\omega_x Q_y - \omega_y Q_x)$ is the spin precession of the spin polarization in the presence of a magnetic field, $\dot{Q}_z\Big|_{sf}$ is the contribution to the time rate of change of the spin polarization due to spin flip processes and, $\dot{Q}_z\Big|_{R+NR}$ is the contribution to the time rate of change of the spin polarization due to recombination. In order to show explicitly the last two therms $\dot{Q}_z\Big|_{sf}$ and $\dot{Q}_z\Big|_{R+NR}$ we have first

$$\dot{Q}_z\Big|_{sf} = \frac{1}{2}\left(-\dot{\rho}_{11}|_{sf} - \dot{\rho}_{-1-1}|_{sf} + \dot{\rho}_{22}|_{sf} + \dot{\rho}_{-2-2}|_{sf}\right). \tag{71}$$

Then, using the explicit derivatives of earlier result in the Tables leads to

$$\begin{aligned} = \frac{1}{2}\Bigg[&\rho_{11}\left(\frac{1}{2\tau_e} + \frac{1}{2\tau_h}\right) - \frac{\rho_{22}}{2\tau_e} - \frac{\rho_{2-2}}{2\tau_h} + \rho_{-1-1}\left(\frac{1}{2\tau_e} + \frac{1}{2\tau_h}\right) \\ &- \frac{\rho_{-2-2}}{2\tau_e} - \frac{\rho_{22}}{2\tau_h} - \rho_{22}\left(\frac{1}{2\tau_e} + \frac{1}{2\tau_h}\right) + \frac{\rho_{11}}{2\tau_e} + \frac{\rho_{-1-1}}{2\tau_h} \\ &- \rho_{-2-2}\left(\frac{1}{2\tau_e} + \frac{1}{2\tau_h}\right) - \frac{\rho_{-1-1}}{2\tau_e} + \frac{\rho_{11}}{2\tau_h}\Bigg]. \end{aligned} \tag{72}$$

Additionally

$$\begin{aligned} \dot{Q}_z\Big|_{R+NR} &= \frac{1}{2}\left(-\dot{\rho}_{11}|_R - \dot{\rho}_{-1-1}|_R\right) + \frac{1}{2}\left(\dot{\rho}_{22}|_{NR} + \dot{\rho}_{-2-2}|_{NR}\right) \\ &= \frac{1}{2\tau_R}\left(\rho_{11} + \rho_{-1-1}\right) - \frac{1}{2\tau_{NR}}\left(\rho_{22} + \rho_{-2-2}\right) \end{aligned} \tag{73}$$

Then, remembering that $\rho_{11} + \rho_{-1-1} = N_b$, $\rho_{22} + \rho_{-2-2} = Nd$, and $Q_z = \frac{Nd - N_b}{2}$ and

using again the generation functions

$$\dot{Q}_z\Big|_{\text{gen}} = \frac{1}{2}\left(-G_{11} - G_{-1-1} + G_{22} + G_{-2-2}\right), \tag{74}$$

one obtains

$$\begin{aligned}\frac{dQ_z}{dt} = (\omega_x Q_y - \omega_y Q_x) - Q_z\left(\frac{1}{\tau_e} + \frac{1}{\tau_h}\right) + \frac{Nb}{2\tau_R} - \frac{Nd}{2\tau_{NR}} \\ - \frac{G_{11} + G_{-1-1}}{2} + \frac{G_{22} + G_{-2-2}}{2}\end{aligned} \tag{75}$$

If the generation rates of excitons with different spin states are different, then the total number of excitons must change by optical pumping. For example, if the generation rate of excitons with spin up is higher than the generation rate of excitons with a down spin, then the total number of excitons will increase over time towards up spin state.

The total number of excitons can be defined as

$$N \equiv \rho_{11} + \rho_{-1-1} + \rho_{22} + \rho_{-2-2}, \tag{76}$$

and their dynamics is modeled by

$$\frac{dN}{dt} = \frac{dN}{dt}\bigg|_{sf} + \frac{dN}{dt}\bigg|_{R+NR} + \frac{dN}{dt}\bigg|_{Gen}. \tag{77}$$

As the terms in $\frac{dN}{dt}\Big|_{sf}$ cancel then

$$\frac{dN}{dt} = G_{11} + G_{-1-1} + G_{22} + G_{-2-2} - \frac{N_b}{\tau_R} - \frac{Nd}{\tau d}. \tag{78}$$

In turn,

$$\frac{dN_d}{dt} - \frac{dN_b}{dt} = 2\left(\omega_x Q_y - \omega_y Q_x\right) - 2Q_z\left(\frac{1}{\tau_e} + \frac{1}{\tau_h}\right) + \frac{N_b}{\tau_R} - \frac{N_d}{\tau_{NR}} - \left(G_{11} + G_{-1-1}\right) + \left(G_{22} + G_{-1-2}\right). \tag{79}$$

This equation describes the rate of change of the number of excitons with dark and bright spin. The first part of the equation, $2\left(\omega_x Q_y - \omega_y Q_x\right)$, describes the spin rotation of the excitons due to the magnetic field. The second part of the equation, $2Q_z\left(\frac{1}{\tau_e} + \frac{1}{\tau_h}\right)$ describes the spin relaxation of excitons for electrons and holes. The third part of the equation, $\frac{N_b}{\tau_R} - \frac{N_d}{\tau_{NR}}$ describes exciton recombination. The last part of the equation describes the generation of excitons with different spin states. So, to describe how the quantity Nd changes over time, taking into account the influence of angular frequencies, spin polarization, relaxation processes, the total number of excitons, and generation processes we can write

$$\frac{2dN_d}{dt} = 2\left(\omega_x Q_y - \omega_y Q_x\right) - 2Q_z\left(\frac{1}{\tau_e} + \frac{1}{\tau_n}\right) - \frac{2Nd}{\tau_{NR}} + 2\left(G_{22} + G_{-2-2}\right). \tag{80}$$

That can be rearranged more conveniently as

$$\frac{dN_d}{dt} = \left(G_{22} + G_{-2-2}\right) - \frac{N_d}{\tau_{NR}} - Q_z\left(\frac{1}{\tau_e} + \frac{1}{\tau_h}\right) + \left(\omega_x Q_y - \omega_y Q_x\right). \tag{81}$$

Now, in the case of the rate of change of the total number of bright excitons, N_b, we have

$$\frac{2dN_b}{dt} = -2\left(\omega_x Q_y - \omega_y Q_x\right) + 2Q_z\left(\frac{1}{\tau_e} + \frac{1}{\tau_n}\right) - \frac{2N_b}{\tau_R} + 2\left(G_{11} + G_{-1-1}\right). \tag{82}$$

This can be rewrite as follows

$$\frac{dN_b}{dt} = \left(G_{11} + G_{-1-1}\right) - \frac{N_b}{\tau_R} + Q_z\left(\frac{1}{\tau_e} + \frac{1}{\tau_h}\right) - \left(\omega_x Q_y - \omega_y Q_x\right) \tag{83}$$

Now, the change rate of the x component of the electron spin magnetic moment within the excitons, under the influence of an external magnetic field can be written as

$$\frac{dS_x}{dt} = (\omega_y S_z - \omega_z S_y) + \tilde{\delta} Q_y + \frac{1}{2}\left(\dot{\rho}_{11} + \dot{\rho}_{21} + \dot{\rho}_{-1-2} + \dot{\rho}_{-2-1}\right)\Big|_{\text{inco}} \tag{84}$$

By using the results condensed in the Tables

$$\begin{aligned}\left.\frac{dS_x}{dt}\right|_{sf} = \frac{1}{2}\Bigg(&\frac{\rho_{11}}{\tau_e} - \frac{\rho_{12}}{2\tau_h} + \frac{\rho_{-2-1}}{2\tau_h} - \frac{\rho_{21}}{\tau_e} - \frac{\rho_{21}}{\tau_h} + \frac{\rho_{21}}{2\tau_h} + \frac{\rho_{-1-2}}{2\tau_h} - \frac{\rho_{-1-2}}{\tau_e} \\ &- \frac{\rho_{-1-2}}{2\tau_h} + \frac{\rho_{21}}{2\tau_h} - \frac{\rho_{-2-1}}{\tau_e} - \frac{\rho_{-2-1}}{2\tau_h} + \frac{\rho_{12}}{2\tau_h}\Bigg)\end{aligned} \tag{85}$$

That simplifies under the following assumptions: the spin-flip relaxation rate for bright excitons is equal to the spin-flip relaxation rate for dark excitons and the spin-flip relaxation rate for bright excitons is equal to the rate of radiative and non-radiative exciton recombination. As a result, it is seen that the rate of change of the x component of the spin magnetic moment due to the spin-flip relaxation processes is proportional to the spin magnetic moment and the spin-flip relaxation time.

$$\begin{aligned}\left.\frac{dS_x}{dt}\right|_{sf} &= \frac{1}{2\tau_e}\left(-\rho_{12} - \rho_{21} - \rho_{-1-2} - \rho_{-2-1}\right) \\ &= \frac{-S_x}{\tau_e}.\end{aligned} \tag{86}$$

By considering now the radiative and no radiative processes, we have

$$\begin{aligned}\left.\frac{dS_x}{dt}\right|_{R+NR} = \frac{1}{2}\Bigg[&-\rho_{12}\left(\frac{1}{2\tau_R} + \frac{1}{2\tau_{NR}}\right) - \rho_{21}\left(\frac{1}{2\tau_R} + \frac{1}{2\tau_{NR}}\right) \\ &-\rho_{-1-2}\left(\frac{1}{2\tau_R} + \frac{1}{2\tau_{NR}}\right) + \rho_{-2-1}\left(\frac{1}{2\tau_R} + \frac{1}{2\tau_{NR}}\right)\Bigg]\end{aligned} \tag{87}$$

This last equation simplifies to

$$\left.\frac{dS_x}{dt}\right|_{R+NR} = -S_x\left(\frac{1}{2\tau_R} + \frac{1}{2\tau_{NR}}\right) \tag{88}$$

The complete rate of change of the x component of the spin magnetic moment of excitons is

$$\frac{dS_x}{dt} = -S_x\left(\frac{1}{\tau_e} + \frac{1}{2\tau_R} + \frac{1}{2\tau_{NR}}\right) + (\omega_y S_z - \omega_z S_y) + \tilde{\delta} Q_y \tag{89}$$

Radiative recombination is when an exciton recombines and emits a photon. Nonradiative recombination is when an exciton recombines without emitting a photon.

The following equations in Table IV describes the complete rate of change of the y-components of the exciton spin magnetization, taking into account the same factors as in previous terms. The first column of the table shows the name of the derivative, the second column shows the mathematical expression for the derivative. The third column provides a brief description of the contribution of each term to the derivative.

TABLE IV: Derivatives of the y component of the spin magnetic moment of the excitons in a semiconductor, under the influence of an external magnetic field and spin-flip relaxation processes.

$\frac{\#}{dt}\Big\vert$	Expression	Description
$\frac{dS_y}{dt}\Big\vert_{sf}$	$-\frac{S_y}{\tau_e}$	Spin-flip relaxation
$\frac{dS_y}{dt}\Big\vert_{R+NR}$	$-S_y\left(\frac{1}{2\tau_R} + \frac{1}{2\tau_{NR}}\right)$	Rad. and non-rad. recomb.
$\frac{dS_y}{dt}$	$-S_y\left(\frac{1}{\tau_e} + \frac{1}{2\tau_R} + \frac{1}{2\tau_{NR}}\right) + (\omega_z S_x - \omega_x S_z) - \tilde{\delta} Q_x$	Total derivative
$\frac{dQ_x}{dt}\Big\vert_{sf}$	$-Q_x\left(\frac{1}{\tau_e} + \frac{1}{\tau_h}\right)$	Spin-flip relaxation
$\frac{dQ_x}{dt}\Big\vert_{R+NR}$	$-Q_x\left(\frac{1}{2\tau_R} + \frac{1}{2\tau_{NR}}\right)$	Rad. and non-rad. recomb.
$\frac{dQ_x}{dt}$	$-Q_x\left(\frac{1}{2\tau_R} + \frac{1}{2\tau_{NR}} + \frac{1}{\tau_e} + \frac{1}{\tau_h}\right) + (\omega_y Q_z - \omega_z Q_y) + \tilde{\delta} S_y$	Total derivative
$\frac{dQ_y}{dt}\Big\vert_{sf}$	$-Q_y\left(\frac{1}{\tau_e} + \frac{1}{\tau_h}\right)$	Spin-flip relaxation
$\frac{dQ_y}{dt}\Big\vert_{R+NR}$	$-Q_y\left(\frac{1}{2\tau_R} + \frac{1}{2\tau_{NR}}\right)$	Rad. and non-rad.recomb.
$\frac{dQ_y}{dt}$	$-Q_y\left(\frac{1}{2\tau_R} + \frac{1}{2\tau_{NR}} + \frac{1}{\tau_e} + \frac{1}{\tau_h}\right) + (\omega_z Q_x - \omega_x Q_z) - \tilde{\delta} S_x$	Total derivative

The derivatives of the y-component of the exciton spin moment can be divided into two categories: spin-flip relaxation (sf) and radiative and non-radiative recombination (R+NR). Spin-flip relaxation derivatives describe the decay of the y-component of the exciton spin moment due to spin-flip processes. Spin-flip processes can occur between excitons with different spin states.

VI. RESULTS

A. Spin polarization

In the context of our study, the exciton polarization can be used to determine the preferential orientation of the spins of electrons and holes in response to a magnetic field and all the dynamic processes just described. Under stationary conditions, all the time derivatives in the tables and equation above can be considered zero and the spin polarizations can be assessed.

We have been able to reproduce the main result of Ref. [9] that characterizes the electron polarization that can be defined as the difference between available electrons with spin up, $\rho_{22} + \rho_{-1-1}$ and spin down, $\rho_{11} + \rho_{-2-2}$, weighted by the total number of available electrons $\rho_{11} + \rho_{-1-1} + \rho_{22} + \rho_{-2-2} = N_b + N_d$. This yields, according to Eq. 35

$$P_e = \frac{2\langle S_z \rangle}{\langle N_b + N_d \rangle}. \tag{90}$$

In Ref. [9], beside the effect of the external field, B_z, they have included the contribution to the effective magnetic field of the nuclear spins randomized following a Gaussian distribution with dispersion Δ_B. After some cumbersome algebra and by neglecting all direct spin-flip terms one gets that

$$P_e = \frac{-2B_z B_{exch}}{B_z^2 + B_{\text{exch}}^2 + \Delta_B^2}, \tag{91}$$

where $B_{exch} = \delta_0/g_e\mu_B$. This is a relevant result that points to the fact that the bright to dark exciton correlation leads to a net non-zero electron spin polarization as we can see in Figs. 6. Note that, in absolute terms, this results is very similar to the experiment described in Fig. 1. Indeed, the curves that fit those values use this same expression and we should come back to that later.

The polarization of electrons in confined excitons is a complex function of the magnetic field and the parameters B_{exch} and Δ_B. In Fig. 6 we get the variation of polar-

ization as a function of B_z while B_{exch} and Δ_B are kept constant. The polarization is maximized when the magnetic field approaches $B_z = \sqrt{B_{exch}^2 + \Delta_B^2}$ and collapses to zero when the magnetic fields increases beyond that point. This is a contrast with the thermal polarization that is expected to reach a saturation as the field increases.

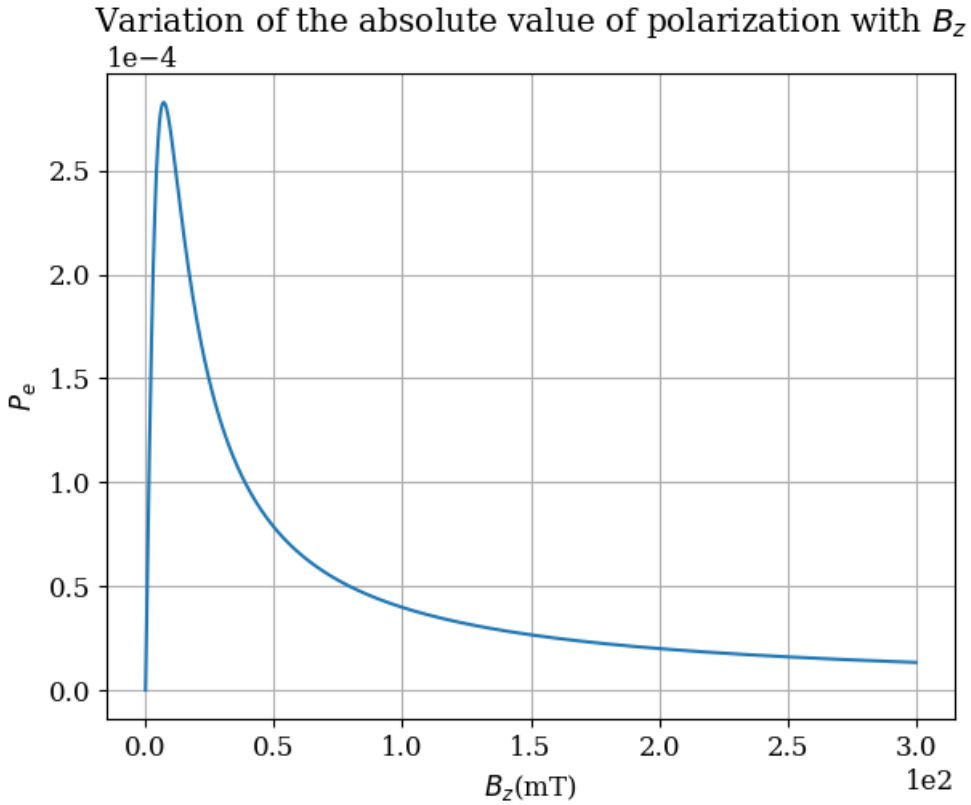

FIG. 6: The spin polarization of the electrons as a function of the external magnetic field, B_z , for a constant exchange magnetic field, $B_{exch} = 0.5mT$. The spin polarization increases when B_z approaches to B_{exch} .

Then, in Fig. 7, we modeled the variation of the electron polarization with respect to Δ_B, with B_z and B_{exch} constants. This illustrates how the electron polarization is affected by changes in the dispersion of nuclear spins, Δ_B. We can note that the maximum polarization always appears as $\Delta_B \Rightarrow 0$, when the dispersion is sharper, while disappearing if the nuclear spins are widely randomized.

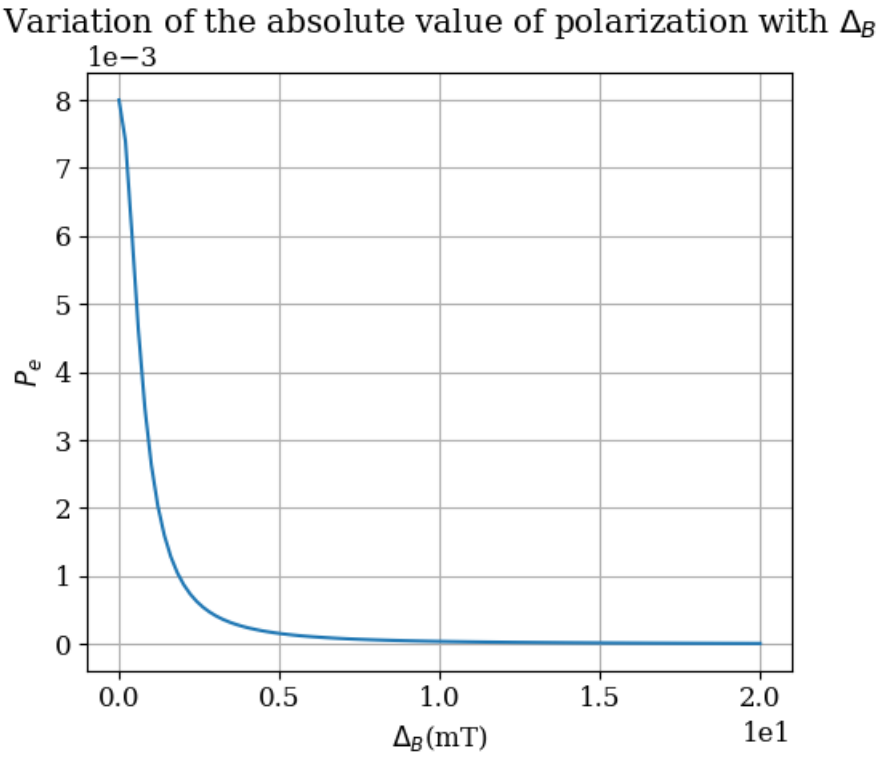

FIG. 7: Variation of the absolute value of polarization with Δ_B. This graph shows how the absolute value of the polarization of the electrons in a semiconductor varies as a function of the variation in nuclear spin dispersion Δ_B. Absolute polarization is a measure of the deviation of the electron distribution from thermal equilibrium in the presence of a magnetic field. As the value of Δ_B increases, the polarization of the electrons tends to decrease and to approach zero.

Now in Fig. 8 we see how the polarization behaves simultaneously for a range of values of the B_{exch} and the Δ_B. A symmetrical behavior is obtained around the zero exchange field value (vertical axis), while we also observe that the polarization decreases as the Δ_B increases much beyond 0.5 mT.

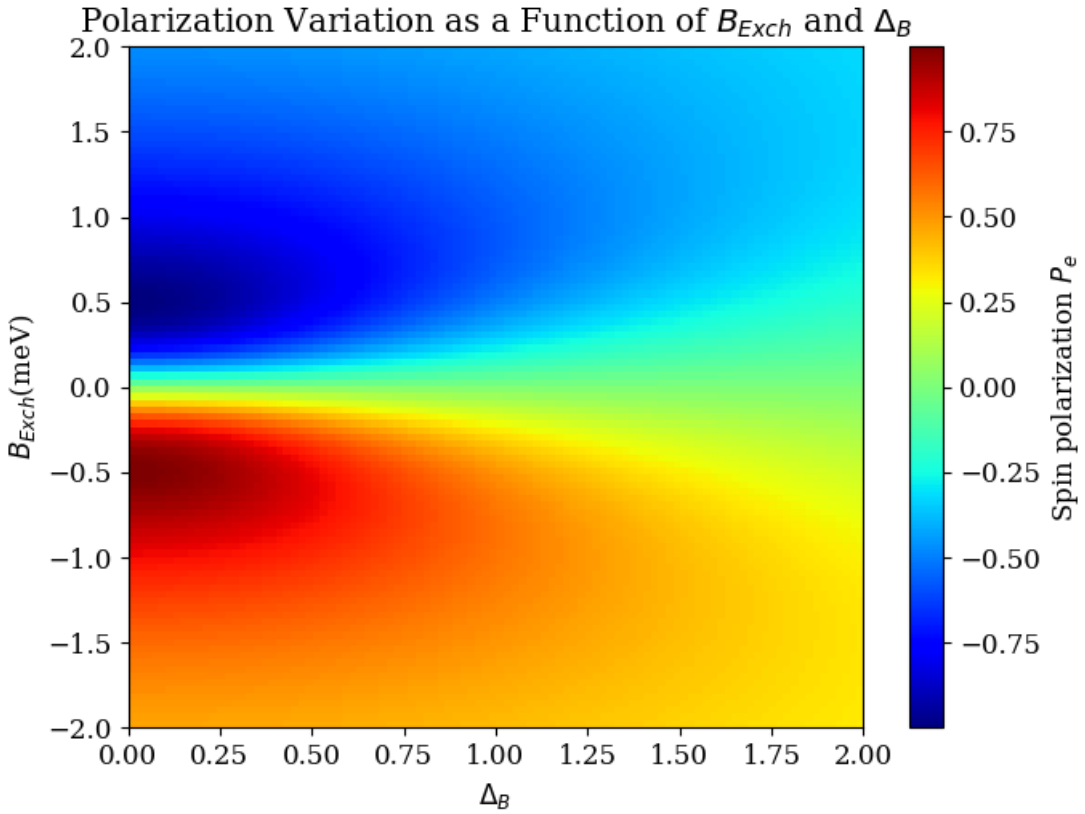

FIG. 8: Polarization Variation as a Function of B_{Exch} and Δ_B. This 2D colormap depicts the absolute value of electron polarization as a function of the exchange magnetic field B_{Exch} and the nuclear spin dispersion Δ_B. Darker regions indicate higher polarization, while lighter areas represent lower polarization(opposite directions). The graph provides insights into the intricate interplay between these magnetic parameters and their influence on electron polarization in the semiconductor material.

Since half of the polarization values are negative, we chose to represent the polarization in three dimensions so that we can observe the complete dependence of the average orientation of the electron spins in better details, in relation to the B_{exch} field and the Δ_B.

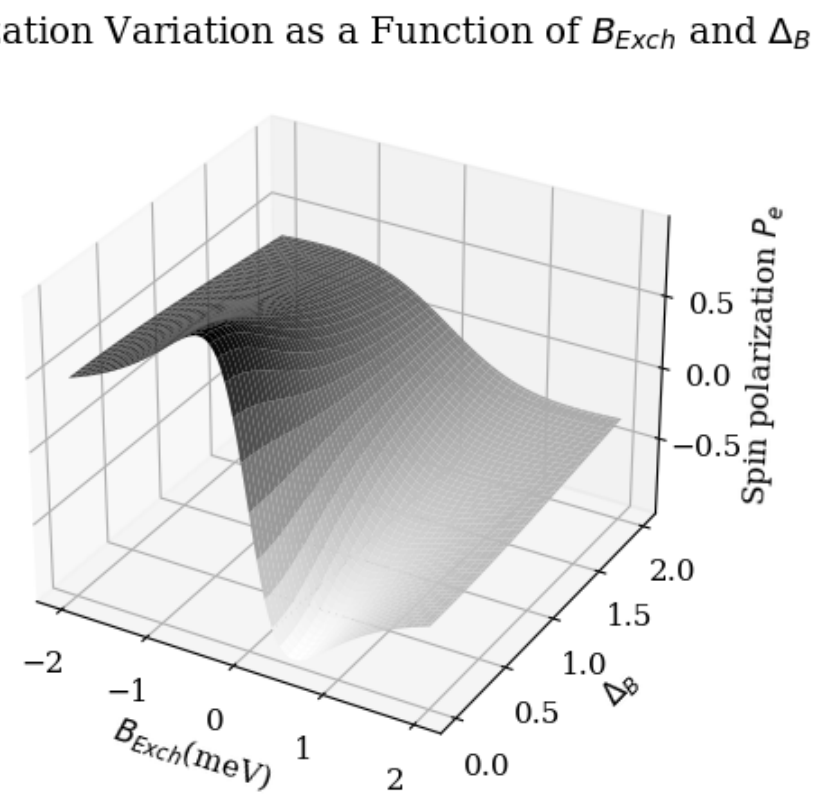

FIG. 9: Polarization vs. B_{Exch}, Δ_B. This three-dimensional graph represents the polarization of the electronic spins as a function of two variables: the exchange magnetic field B_{Exch} and Δ_B. Spin polarization is maximum when external and internal magnetic fields are equal

The dependence on magnetic field B_z that we observe in Fig. 6 is consistent with Fig. 1. In our case we use the polarization in absolute value to reproduce the version proposed in Ref. [9]. The questions arises on whether the measured exciton polarization in the experiment of Fig. 1 corresponds to the electron polarization just described.

However, we have also been able to calculate the polarization of bright excitons which can be directly related to the degree of circular polarization that can be measured in the PL emission. In this case it would be defined as

$$P_{PL} = \frac{\langle J_z/3 - S_z \rangle}{\langle N_b \rangle}. \tag{92}$$

Then, by using the same exact approximations reported in Ref. [9], we have calculated the value of $P_{PL} = 0$ that exactly cancels out for any value of the magnetic field. This is relevant because clearly the approximations used in Ref. [9] are too strong for emulating the polarized emission of the PL reported experimentally in our experiments. Thus, under these assumptions the polarization described in the experiments of Fig. 1, cannot be related to the electron polarization nor to any exciton polarization ascribed to the hyperfine interaction and contribution of nuclear spins.

B. Termalization

By assuming now the possibility of thermal equilibrium, we are able to also characterize the spin polarization. We will assumed the 2D density of excited electron-hole pairs as a known parameter n_{2D} thus using Eq. (16) one gets the following results, as reported in Ref. [1]

$$2\pi\frac{\hbar^2}{m_0}n_{2D} = \hbar\omega_c^0\sum_{N,s} f\left[\frac{\hbar\omega_c^0}{m^*}\left(N+\frac{1}{2}\right)+\frac{s}{4}\cdot g\hbar\omega_c^0,\mu\right], \tag{93}$$

with $\omega_c^0 \equiv \frac{eB}{m_0 c}$, where

$$f(E,\mu) = \frac{1}{1+\exp\left(\frac{E-\mu}{k_B T_{eff}}\right)} \tag{94}$$

is the Fermi-Dirac distribution for certain effective temperature, T_{eff}. We can then use Eq. (94) to calculate the Fermi level tuning with magnetic field for a given value of temperature and electron density. This has been illustrated in Fig. 10 and Fig.11 that shows how the Landau levels fill up in relation to the Fermi level, in such a way that the probability of occupation can be obtained for each of them. It can be seen how by increasing the effective temperature, which should not necessarily be the lattice temperature [30], the curves are less defined, and the Landau level filling begins to blur. That is to say, having a lower temperature, a sharper filling is observed and therefore the shape of a chainsaw appears.

We present the result of the model that shows how electrons in a confined 2D system respond to the presence of a magnetic field, generating quantized energy levels known as Landau levels Fig.11. The graph illustrates how these levels fill according to the Fermi distribution as the magnetic field strength is varied. The underlying physics is a manifestation of the quantization of energy in quantum systems and the fermionic character of the electrons.

As we can see in graphs 10 and 11, the interesting behavior of the electrons is observed when saturating the initial Landau levels, however, for the sake of the precision of the numerical calculation, several dozens Landau levels were taken into account, to obtain a definition high in the numerical solution in the calculation of the Fermi level.

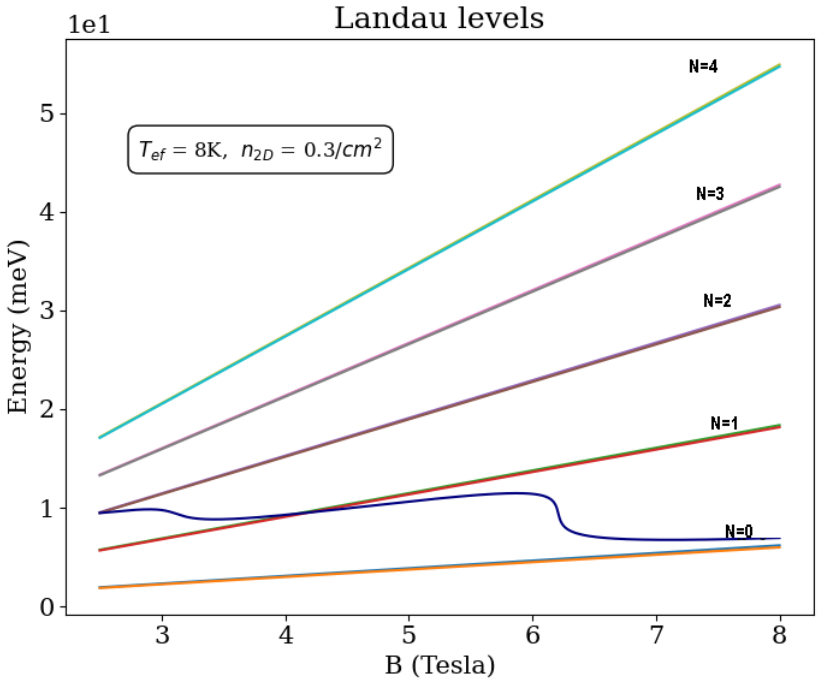

FIG. 10: Graphic representation of the Landau Levels and Fermi Distributions for electrons in a semiconductor exposed to a magnetic field. The effective temperature is $T_{ef} = 8$ K, the two-dimensional density is $n_{2D} = 0.3 \times 10^{12} cm^{-2}$ and the number of Landau levels considered is 5, however the relevant behavior occurs in the first three levels. Landau levels are plotted as a function of magnetic field, revealing relationships between energy and magnetic field, while Fermi distributions for different Landau levels and spins are presented as a function of energy.

In general we have that, when applying a magnetic field, both electrons and holes in a 2D system experience quantization, and the Fermi distribution determines how these levels are filled Fig10 and fig 11. The main difference between electrons and holes is their electrical charge, their effective masses and effective Lande factors that affect their behavior in a magnetic field. In the case of holes, we will observe how they move to higher energy levels as the magnetic field increases and how they fill with increasing effective temperature.

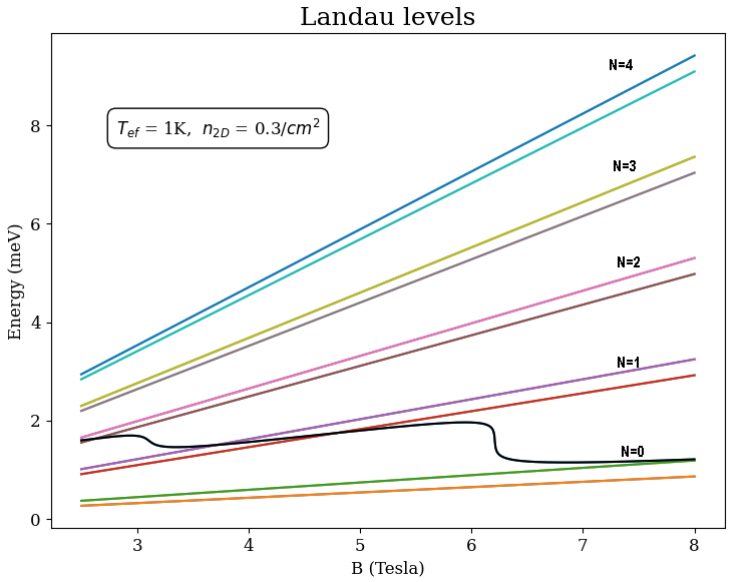

FIG. 11: Simulation of Landau Levels and Fermi Distributions for Holes in a Magnetic Field. This figure shows the simulation of Landau levels and Fermi distributions for holes in a semiconductor under the influence of a magnetic field. Parameters used in the simulation include an effective temperature of $T_{ef} = 1K$, a two-dimensional density of $n_{2D} = 0.3 \times 10^{12}\text{cm}^{-2}$ and a number of Landau levels of 5. The holes are characterized by an effective mass of $m = 0.45$ and a Landé factor of $g = 0.7$. The Landau levels are represented as a function of the magnetic field B in Tesla, and the corresponding Fermi distributions are presented in terms of energy (meV). The adjusted effective temperature (lower than for electrons) allows to capture the subtleties of the effects of effective mass and thermal properties on holes, generating an accurate representation of their behavior under the influence of a magnetic field. The numbers next to the Landau level lines indicate their corresponding indices.

While two-dimensional representations can be useful for visualizing simpler data

and relationships, in cases where a deep and complete understanding of the system is needed, three-dimensional representation offers a significant advantage. 3D data allows us to better explore and understand relationships and effects in complex systems.

A three-dimensional graph is created to represent the results. A two-dimensional grid of B and n_{2D} is created, and then the three-dimensional Fermi surface is represented. The Fermi surface is now calculated and visualized in an electronic system as a function of three variables: magnetic field, two-dimensional density and effective temperature. This 3D representation provides a detailed view of how the Fermi energy changes in response to different system conditions.

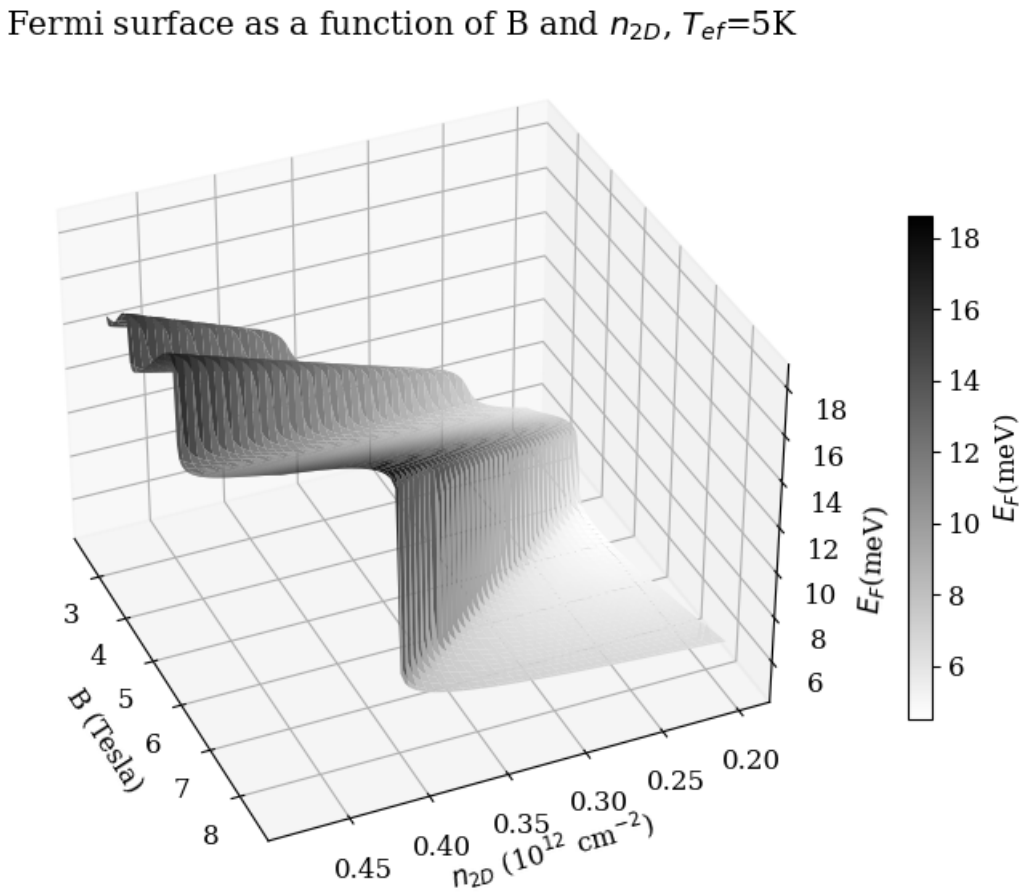

FIG. 12: Fermi surface for confined electrons in the presence of a magnetic field. The ripples on the Fermi surface are caused by the different Landau levels. The density controls the resolution of the Fermi surface. The higher the density, the sharper the edges of the surface.

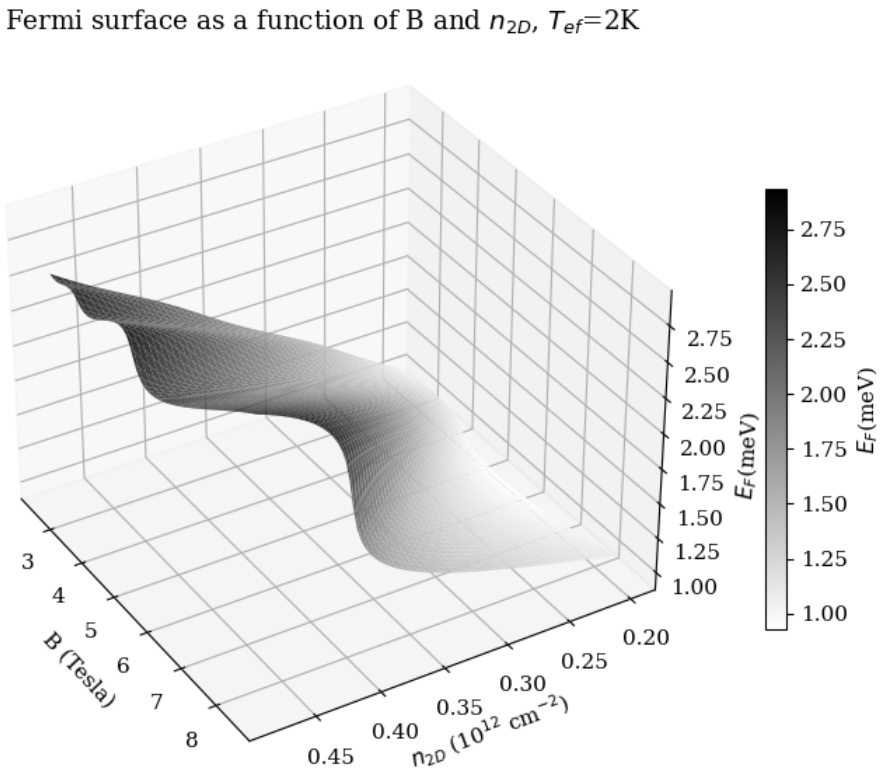

FIG. 13: Fermi surface of holes of a semiconductor material in the presence of a magnetic field. This figure illustrates the three-dimensional variation of the Fermi surface in a two-dimensional semiconductor under the influence of a magnetic field B, and the bi-dimensional density n_{2D} .

Now we shift to a different 3d representation, in Fig. 14 that shows the relations of the Fermi energy an two independent variables, the magnetic field (B) and the effective temperature T_{eff}. This provides a more complete view of how these two variables change and their influence on the Fermi energy. We can also observe this relationship in Fig. 15 as a different view of figure 14.

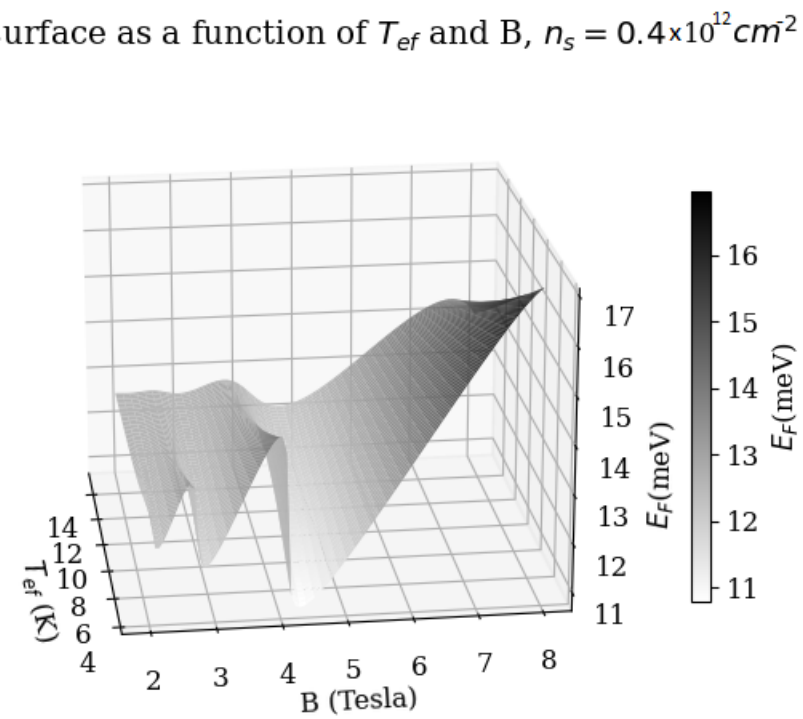

FIG. 14: View 1. Fermi Surface of electrons in a Two-Dimensional Semiconductor model as a Function of Effective Temperature and Magnetic Field. The plot shows the Fermi energy as a series of wavy surfaces where the ripples are caused by the different Landau levels. This figure illustrates the three-dimensional variation of the Fermi surface in a two-dimensional semiconductor under the influence of a magnetic field, as a function of the effective temperature T_{eff} and the magnetic field (B). Colors represent Fermi energy levels E_F in meV. The two-dimensional density $n_{2D} = 0.4x10^{12}cm^{-2}$.

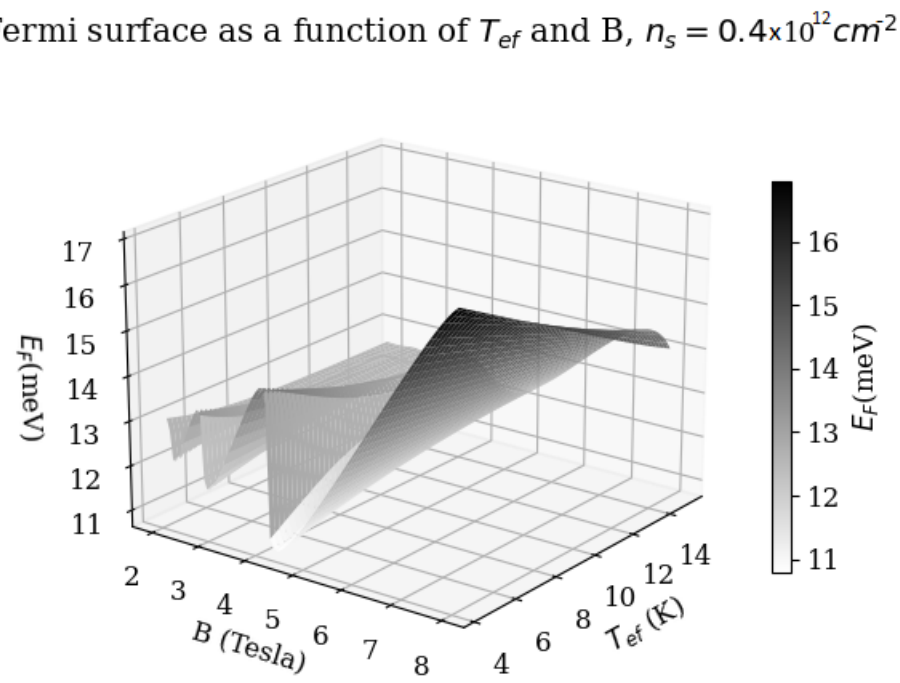

FIG. 15: View 2. We can see how the increment of magnetic field and with low effective temperature allows the electrons to occupy higher energy levels. Each point on the Fermi surface represents the Fermi energy for a specific combination of T_{eff} and B. The colors on the graph represent the variation in Fermi energy: darker colors correspond to higher Fermi energy values and lighter colors at lower values. The color bar on the side of the graph acts as a guide to understand the correspondence between colors and energy values. You can see how the Fermi energy values change as you adjust the temperature and magnetic field.

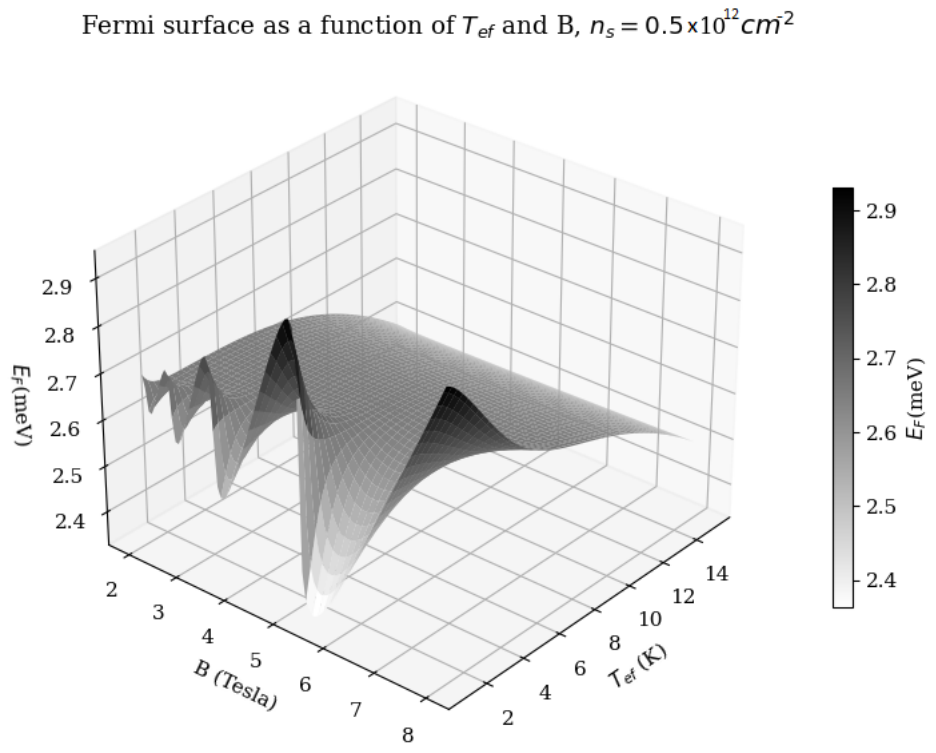

FIG. 16: Fermi Surface in a Two-Dimensional Semiconductor as a Function of T_{eff} and B to holes with Landé factor 0.7 and effective mass 0.45. This three-dimensional graph shows the variation of the Fermi surface in a two-dimensional semiconductor as a function of the effective temperature T_{eff} and the magnetic field B to a fix bi dimensional density $n_{2D} = 0.5 \times 10^{12}\text{cm}^{-2}$.

The function in Fig. 16 has been obtained for a different 2D electron density, modifying the shape of the Fermi surface with respect to the previous ones. It shows that increasing the density of electrons in the semiconductor higher Landau levels are occupied for lower fields.

Let us now analyze how this occupation of quantized levels may affect the electronic structure. For that purpose we will reduce the analysis to the ground state of Eq. 16, and take

$$\widetilde{E}_{0,s} = \frac{s}{4} \cdot g\hbar\omega_c^0. \tag{95}$$

This allows defining the Zeeman spin splitting as $\Delta E_z = \widetilde{E}_{0,+} - \widetilde{E}_{0,+}$. The Zeeman

splitting, under this approximation, increases linearly with the magnetic field. The slope of the line is equal to the Landé factor of the electrons, which is -0.44 in this case.

In this next simulation, the Landau equation and the Fermi-Dirac distribution are used to model this behavior as a function of the effective temperature and magnetic field intensity.

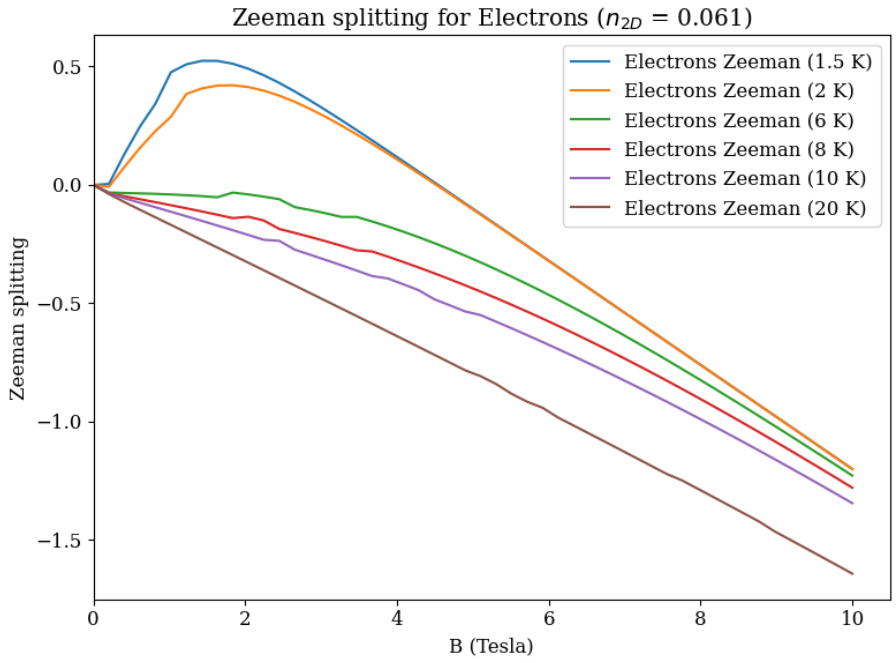

FIG. 17: Zeeman Splitting in Electrons at Effective Temperatures: 1.5 K, 2 K, 6K, 8 K, 10 K, and 20 K, with a 2D density of $n_{2D} = 0.061 \times 10^{12}\text{cm}^{-2}$. The value of the Landé factor for electrons is -0.44 and the effective mass is 0.0760 [31]

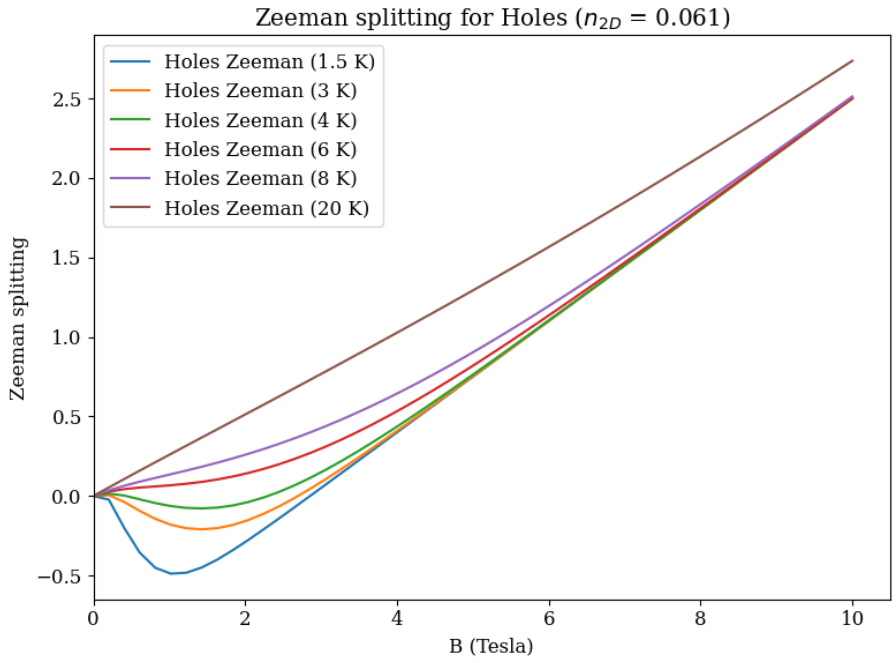

FIG. 18: Graph of the Zeeman Effect in Holes: The graphical representation shows the Zeeman splitting in holes in a semiconductor. Each curve corresponds to a different effective temperature (in this case, 1.5K, 3K, 4K, 6K, 8K, 20K), and shows how the Zeeman splitting varies as the magnetic field increases. The value of the Landé factor for the holes is 0.7 [31] and the effective mass is 0.45

Also we will assume in this case the exchange contribution to the energy state

$$\widetilde{E}_{0,s} = \frac{s}{4} \cdot g\hbar\omega_c^0 + \frac{1}{3}\delta_0 s \cdot \langle j_z \rangle \,. \tag{96}$$

but in terms of a mean value of the hole spin $\langle j_z \rangle$

$$\langle j_z \rangle = \frac{n_{\uparrow\frac{1}{2}} - n_{\downarrow\frac{1}{2}}}{n_\uparrow + n_\downarrow} \approx \frac{1}{2} \frac{f\left(\widetilde{E}_{0,+1}(B), \mu\left(B, T_{eff}\right)\right) - f\left(\widetilde{E}_{0,-1}(B), \mu\left(B, T_{eff}\right)\right)}{f\left(\widetilde{E}_{0,+1}(B), \mu\left(B, T_{eff}\right)\right) + f\left(\widetilde{E}_{0,-1}(B), \mu\left(B, T_{eff}\right)\right)} \tag{97}$$

which, in the first order approximation, can be calculated as

$$\langle j_z \rangle \approx \frac{1}{2} \frac{f\left(E_{0,+1}(B), \mu\left(B, T_{eff}\right)\right) - f\left(E_{0,-1}(B), \mu\left(B, T_{eff}\right)\right)}{f\left(E_{0,+1}(B), \mu\left(B, T_{eff}\right)\right) + f\left(E_{0,-1}(B), \mu\left(B, T_{eff}\right)\right)} \tag{98}$$

The model describes the behavior of a thermalized system of excitons and assumes a relation between the effective temperature, external magnetic field, and the way as the excitons reach equilibrium. It also includes possible asymmetries between the spins up and down, due to the correction provoke by the term $\langle j_z \rangle$. This has been illustrated in Fig. 17 and Fig.18 As we can see the results of our theoretical model, that assumes an eventual spin thermalization of the bright excitons that agrees with the experimental behavior observed in Fig. 2.

The horizontal axis in Fig. 17 represents the magnetic field in Tesla, while the vertical axis represents the Zeeman splitting. It also shows that the Zeeman splitting depends on the effective temperature, at lower effective temperatures the effect of the exchange contribution to the Zeeman splitting is larger. This is because at lower temperatures, there are fewer electrons in the higher energy states, becoming thus highly polarized. As the temperature increases the polarization gets more diffuse and the effect is reduced converging towards the linear behavior of the unperturbed Zeeman splitting.

Figure. 17 illustrates the analogous effect for the Zeeman splitting of confined holes. This effect describes how holes behave in response to an applied magnetic field in the presence of the exchange interaction with electrons. The phenomenon is modeled using the Landau equation and the Fermi-Dirac distribution, allowing us to understand how holes change their behavior with magnetic field intensity and effective temperature.

VII. CONCLUSIONS

The fluctuation of the circular polarization of the exciton emission, described in Fig. 1, cannot be explained within the scope of the model and approximations reported in Ref. [9]. However, this model provides a useful tool to characterize the dynamic electron polarization that arises from the interplay of fine structure and the interaction with nuclear spins. Further calculations must be performed relaxing the parameter constraints to check whether the experimental results can be explained that way.

The spin dynamics of confined excitons in the presence of a magnetic field can be tuned by both the temperature and incident power in a very peculiar way. The experimental observation can be so far be interpreted as the correlation of Zeeman splitting, exchange interaction, and spin thermalization. Our findings indicate that the incident power exerts a significant influence on the exciton spin dynamics. Varying the incident power reveals distinctive patterns in the evolution of spin polarization, thus providing a tunable tool to control and manipulate quantum information in these systems.

The experimental observation of the Zeeman splitting correlation in our results supports the idea that the presence of a magnetic field triggers notable changes in the spin structure of excitons. This phenomenon offers a valuable tool for probing and controlling quantum states in nanostructured systems.

Advanced understanding of spin dynamics in confined excitons opens new possibilities for technological applications[32]. These results could have implications for the development of quantum devices, such as quantum qubits, and components for emerging technologies based on the manipulation of quantum states.

[1] G. Bastard, enWave mechanics applied to semiconductor heterostructures, Wiley series in monographs of physics (John Wiley & Sons, Nashville, TN, 1990).

[2] A. V. T. A. S. Kurdyubov, Physical Review B **107**, 024065 (2023).

[3] M. M. Glazov, Electron & nuclear spin dynamics in semiconductor nanostructures, Series on Semiconductor Science and Technology (Oxford University Press, London, England, 2018).

[4] R. C. H. Rair Macêdo, PhysRevApplied.15.024065 **15**, 024065 (2021).

[5] S. B. Prashanth Barla, Vinod Kumar Joshi, Journal of Computational Electronics **20**, 1648 (2021).

[6] E. Blackwood, M. J. Snelling, R. T. Harley, S. R. Andrews, and C. T. B. Foxon, Phys. Rev. B **50**, 14246 (1994).

[7] A. S. Davydov, Quantum mechanics (Pergamon Press, 1976).

[8] A. P. Heberle, W. W. Rühle, and K. Ploog, Phys. Rev. Lett. **72**, 3887 (1994).

[9] D. Smirnov, T. Shamirzaev, D. Yakovlev, and M. Bayer, Physical Review Letters **125** (2020), 10.1103/physrevlett.125.156801.

[10] I. I. Y. I. A. Solovev, Physical Review Applied **15**, 024065 (2022).

[11] E. Margapoti, L. Worschech, S. Mahapatra, K. Brunner, A. Forchel, F. M. Alves, V. Lopez-Richard, G. E. Marques, and C. Bougerol, Phys. Rev. B **77**, 073308 (2008).

[12] R. R. Silva, Pontos quânticos tipo-II cobertos por antimonetos, Trabalho de Conclusão de Curso (Graduação em Engenharia Física) (Universidade Federal de São Carlos, 2022).

[13] H. Ochoa, A. H. C. Neto, and F. Guinea, Physical Review Letters **108** (2012), 10.1103/physrevlett.108.206808.

[14] J. Zhou and M. W. Wu, (2007), 10.48550/ARXIV.0705.0216.

[15] L. C. W. H. L. Y. Zhang, X. and Z. Zhang, RinEnG **5**, 101347 (2023).

[16] in Condensed Matter Physics (John Wiley & Sons,Inc., Hoboken, USA, 2010) pp. 265–292.

[17] P. Y. Yu and M. Cardona, enFundamentals of semiconductors, 4th ed., Graduate texts in physics (Springer, Berlin, Germany, 2010).

[18] M. I. Dyakonov, ed., Spin Physics in Semiconductors (Springer Berlin Heidelberg, 2008).

[19] Y. U. Peter and M. Cardona, enFundamentals of semiconductors, 4th ed., Graduate Texts in Physics (Springer, Berlin, Germany, 2010).

[20] L. D. Landau and E. M. Lifshitz, Quantum mechanics, 3rd ed., edited by J. Menzies (Butterworth-Heinemann, Oxford, England, 1981).

[21] R. Winkler, enSpin-orbit coupling effects in two-dimensional electron and hole systems, Springer tracts in modern physics (Springer, New York, NY, 2003).

[22] P. Puschnig and C. Ambrosch-Draxl, Comptes Rendus. Physique **10**, 504 (2009).

[23] R. P. Prasankumar and A. J. Taylor, Optical Techniques for Solid-State Materials Characterization (John Wiley & Sons, 2012).

[24] G. Isbn, 50 easy contemporary pieces (Mel Bay Publications, Pacific, MO, 2022).

[25] G. E. Pikus and G. L. Bir, Zh. Eksp. Teor. Fiz **60**, 195 (1971).

[26] M. Dyakonov, X. Marie, T. Amand, P. L. Jeune, D. Robart, M. Brousseau, and J. Barrau, Physical Review B **56**, 10412 (1997).

[27] D. G. Tempel, J. Yuen-Zhou, and A. Aspuru-Guzik, in Fundamentals of Time-Dependent Density Functional Theory, Lecture Notes in Physics, Vol. 837, edited by A. Aspuru-Guzik and M. Head-Gordon (Springer, 2012) pp. 211–229.

[28] J. J. Sakurai and J. J. Napolitano, Modern Quantum Mechanics (Addison Wesley, 2010).

[29] E. Ivchenko, V. Kochereshko, A. Naumov, I. Uraltsev, and P. Lavallard, Superlattices and Microstructures **10**, 497 (1991).

[30] E. D. Guarin Castro, A. Pfenning, F. Hartmann, G. Knebl, M. Daldin Teodoro, G. E. Marques, S. Höfling, G. Bastard, and V. Lopez-Richard, The Journal of Physical Chemistry C **125**, 14741 (2021), https://doi.org/10.1021/acs.jpcc.1c02173.

[31] V. Laurindo, E. D. Guarin Castro, G. M. Jacobsen, E. R. C. de Oliveira, J. F. M. Domenegueti, B. Alén, Y. I. Mazur, G. J. Salamo, G. E. Marques, E. Marega, M. D.

Teodoro, and V. Lopez-Richard, Physical Review B **105**, 045414 (2022).

[32] A. Sharma, M. M. Hasan, and Y. Lu, Materials Futures **1**, 042001 (2022).